**Short title: Ophiostomatales from termite-fungus combs**

# Phylogenetic and phylogenomic analyses reveal two new genera and three new species of ophiostomatalean fungi from termite-fungus combs

Wilma J. Nel[a*i], Z. Wilhelm de Beer[a], Michael J. Wingfield[a], Michael Poulsen[b], Duur K. Aanen[c], Brenda D. Wingfield[a], Tuan A. Duong[a*]

[a] Department of Biochemistry, Genetics and Microbiology, Forestry and Agricultural Biotechnology Institute (FABI), University of Pretoria, Private Bag X20, Pretoria, 0028 South Africa; [b] Section for Ecology and Evolution, Department of Biology, University of Copenhagen, DK-2100 Copenhagen, Denmark; [c] Laboratory of Genetics, Arboretumlaan 4, 6703 BD Wageningen, The Netherlands.

## ABSTRACT

The Ophiostomatales (*Ascomycota*) accommodates more than 300 species characterized by similar morphological adaptations to arthropod dispersal. Most species in this order are wood-inhabiting fungi associated with bark or ambrosia beetles. However, a smaller group of species occur in other niches such as in soil and *Protea* infructescences. Recent surveys of *Termitomyces* fungus gardens (fungus combs) of fungus-growing termites led to the discovery of characteristic ophiostomatalean-like fruiting structures. In this study, these ophiostomatalean-like fungi were identified using morphological characteristics, conventional molecular markers and whole genome sequencing. In addition, the influence of the extracts derived from various parts of *Termitomyces* combs on the growth of these fungi in culture was considered. Based on phylogenomic analyses, two new genera (*Intubia* and *Chrysosphaeria*) were introduced to accommodate these Ophiostomatalean species. Phylogenetic analyses revealed that the isolates resided in three well-supported lineages, and these were described as three new species (*Intubia macrotermitinarum, I. oerlemansii* and

*Chrysosphaeria jan-nelii*). Culture-based studies showed that these species do not depend on the *Termitomyces* comb material for growth.

**KEY WORDS:** Fungus growing termites, Insect associated fungi, *Termitomyces*, Ophiostomataceae, 3 new species, 2 new genera

## INTRODUCTION

The Ophiostomatales was first described in the late 1900's to accommodate the single family, Ophiostomataceae, which at the time included *Ceratocystis, Ceratocystiopsis, Ophiostoma,* and *Sphaeronaemella* (Benny & Kimbrough 1980). These genera share morphologically similar ascomata and ascospores that are adapted to arthropod dispersal (Malloch & Blackwell 1993). However, early DNA based phylogenetic studies showed that species of *Ophiostoma* and *Ceratocystis* are not closely related and reside in two different orders (Ophiostomatales and Microascales) of the Sordariomycetes (Hausner et al. 1993; De Beer et al. 2013a). Subsequently, numerous phylogenetic studies of the Ophiostomatales have been done; each including larger numbers of taxa and additional gene regions to address various questions surrounding the taxonomy and generic placement of many species (Spatafora & Blackwell 1994; Jacobs et al. 2001; Zipfel et al. 2006; Massoumi Alamouti et al. 2009; De Beer et al. 2016a).

De Beer & Wingfield (2013) provided an extensive review of the Ophiostomatales based on the "one fungus one name" principles (Hawksworth et al. 2011). Their phylogenetic analyses, including all published Ophiostomatales sequences in NCBI GenBank at the time, recognized six genera. However, the authors concluded that sequences for a greater number of gene regions and species were needed to resolve the generic boundaries of some lineages. Based on various revisions, the order now accommodates 12 genera including *Afroraffaelea*, *Aureovirgo*, *Ceratocystiopsis*, *Estyea*, *Fragosphaeria*, *Graphilbum*, *Grosmannia sensu latu*

(s.l.), *Hawksworthiomyces*, *Leptographium* s.l., *Ophiostoma* s.l., *Sporothrix*, and *Raffaelea* (De Beer et al. 2016a; De Beer et al. 2016b; Bateman et al. 2017).

Most of the genera in the Ophiostomatales, especially *Ophiostoma* s.l., *Leptographium* s.l., *Ceratocystiopsis*, *Grosmannia* and *Graphilbum*, include species that are commonly associated with Scolytine bark beetles or their galleries (Six 2012; De Beer & Wingfield 2013; Kirisits 2013). However, in addition to these bark beetle associates, four other ecologically distinct groups have been identified. Two of these are species of *Raffaelea* and *Afroraffaelea* (De Beer et al. 2013a; Bateman et al. 2017), which are symbionts of ambrosia beetles where they are cultivated within the beetle galleries as a food source (Harrington et al. 2010; Six 2012). Another group of species reside in *Sporothrix* (De Beer et al. 2016a), which are associated with mites, soil, *Protea* infructescences and a few species that are opportunistic human and animal pathogens (De Lima Barros et al. 2004; De Meyer et al; 2008; Roets et al. 2010; Hofstetter et al. 2013). A fourth ecologically distinct group accommodates species of *Hawksworthiomyces*, which appear to have the characteristic ability to break down the constituents that make up wood (De Meyer et al. 2008; De Beer et al. 2016b).

Ascocarps resembling ophiostomatalean fungi were observed on *Macrotermes natalensis* *Termitomyces* fungus combs in previous studies and fungal cultures were successfully isolated from this material. The aims of this study were (1) to identify these ophiostomatalean-like fungi based on conventional molecular markers, whole genome sequencing and morphological characteristics and (2) to consider if extracts of *Termitomyces* combs have an effect on their growth and development.

## MATERIALS AND METHODS

*Fungal isolations.*—

*Termitomyces* combs were incubated in the absence of termites for up to two months, during which they were inspected multiple times for ophiostomatalean-like fruiting bodies. When observed, single spore drops were lifted from the tips of fruiting bodies using sterilized fine-tipped tweezers (Dumont®, Montignez, Switzerland) and transferred onto malt extract agar (MEA) plates containing streptomycin and cycloheximide (2 % malt extract and 2 % Difco® agar, Biolab, Midrand, South Africa, 0.04 % streptomycin and 0.05 % cycloheximide, Sigma-Aldrich, Kempton Park, South Africa). The plates were incubated for 7–10 d at ambient temperature (~20 C) until fungal colonies were visible. The colonies were then inspected and those with ophiostomatalean-like morphology were sub-cultured by transferring hyphal tips from the edge of an actively growing colony to a new MEA plate. The sub-culturing was repeated until pure cultures were obtained. Pure cultures were maintained on MEA and representatives were submitted to the culture collection (CMW) of the Forestry and Agricultural Biotechnology Institute (FABI), University of Pretoria, South Africa and the Westerdijk Fungal Biodiversity Institute (CBS-KNAW), Utrecht, The Netherlands (TABLE 1; SUPPLEMENTARY TABLE 1).

*DNA extraction, PCR, and sequencing.*—

DNA was extracted for all isolates following the protocol described by De Beer et al. (2014). The DNA solutions were used as template for PCR and the remainder were stored at -20 C. Three gene regions were chosen for amplification, sequencing, and phylogenetic analyses. The 28S ribosomal large subunit (LSU) region was amplified using the primers LR0R and LR5 (Vilgalys & Hester 1990), the ITS1-5.8S-ITS2 region (ITS) was amplified using the primers ITS1F (Gardes & Bruns 1993) and ITS4 (White et al. 1990), and the partial beta-tubulin (*β-tubulin*) gene region was amplified using primers T10 (O'Donnell & Cigelnik 1997) and Bt2b (Glass & Donaldson 1995). PCR reactions were carried out as described by Duong et al. (2012) in a 25 µL reaction volume and the annealing temperature was 55 C.

PCR products were treated before sequencing using the ExoSAP-IT™ PCR Product Cleanup Reagent (ThermoFisher Scientific, Waltham, Massachusetts) following the manufacturer's protocols. Sequencing PCR reactions were performed for both forward and reverse primers as used in PCR. The samples were prepared for sequencing per the BIGDYE® TERMINATOR 3.1 Cycle sequencing protocol (ThermoFisher Scientific) using an annealing temperature of 55 C. Products were purified using sodium acetate and ethanol precipitation and submitted for sequencing on an ABI PRISM®3100 Genetic Analyzer (Applied Biosystems, Foster City, California).

*Phylogenetic analyses.*—

Consensus sequences were used for BLAST searches against the NCBI GenBank non-redundant nucleotide sequence database to identify primary taxonomic grouping of the isolates. Based on these groupings, a total of three datasets were prepared for phylogenetic analyses (one LSU, one ITS and one *β-tubulin*). Reference sequences for these datasets were selected based on the phylogenies of De Beer & Wingfield (2013), De Beer et al. (2016 a & b) and downloaded from NCBI GenBank (Treebase Project no: 28436). For the analyses of the *β-tubulin* dataset, the intron and exon regions were determined for the different isolates based on the *β-tubulin* gene map compiled by Yin et al. (2015).

Each dataset was analysed separately due to uneven sequence availability among the different datasets. Alignments were done using the online version of MAFFT 7 (Katoh & Standley 2013) using default settings. The datasets were treated with GBLOCKS 0.91b (Castresana 2000) using the less stringent options to eliminate poorly aligned positions before phylogenetic analysis. Maximum parsimony analyses were performed using MEGA 6.06 (Tamura et al. 2013). Phylogenies were generated using Subtree-Pruning-Regrafting algorithm starting with 10 random initial trees. Alignment gaps and missing data were included. Node confidence levels were tested using 1000 bootstrap replicates. Maximum

likelihood analyses were performed using the software RAXMLGUI 2 (Silvestro & Michalak 2012, Elder et al. 2019). Phylogenies were generated following the GENERAL TIME REVERSIBLE + GAMMA (GTR+G) nucleotide substitution model. Ten parallel runs each with 1000 thorough bootstrap replicates were conducted. Bayesian inference analyses were performed using MRBAYES 3.2.5 (Ronquist & Huelsenbeck 2003). Phylogenies were generated following the MARKOV CHAIN MONTE CARLO (MCMC) method using the GTR+G model. Ten parallel runs, each with four independent MCMC chains were conducted. Trees were sampled every 100$^{th}$ generation for 5 million generations. Estimated sample size (ESS) and potential scale reduction factor (PSRF) values were used to confirm proper sampling and run convergence had been achieved. Trees sampled during the burn-in phase (25 % of trees sampled) were discarded and posterior probabilities were calculated from the remaining trees.

*Genome sequencing.—*

Due to incongruence between phylogenetic analyses of different gene regions and the unique ecology of the isolates obtained from *Termitomyces* combs, we explored the use of phylogenomic methods to clarify the placement of these species within the Ophiostomataceae. To this end, the genomes of two isolates (CMW 47056 and CMW 47058) each representing a newly identified major lineage (referred to as lineage B and A respectively in the analyses) were sequenced and assembled. Single-conidial isolates of cultures CMW 47056 and CMW 47058 were grown in McCartney bottles containing 10 mL malt yeast broth (YM: 2 % malt extract, 0.5 % yeast extract, Biolab, Midrand, South Africa). The mycelium was collected by centrifugation in 2 mL Eppendorf tubes and freeze dried. Genomic DNA was extracted from freeze-dried mycelium using the salt-based extraction method described by Duong et al. (2013). A TruSeq PCR-Free paired-end library (550 bp average insert sizes) was prepared for each isolate and sequenced using the Illumina HiSeq2500 Platform (Macrogen Inc, Seoul, Korea) to obtain 251 bp paired-end reads.

Quality and adapter trimming of pair-end reads was carried out using TRIMMOMATIC 0.36 (Bolger et al. 2014). *De novo* assembly of the genomes were carried out using SPADES 3.9 (Bankevich et al. 2012), followed by scaffolding using SSPACE-STANDARD 3.0 (Boetzer et al. 2011). Assembly gaps were filled or extended using GAPFILLER 1.10 (Boetzer & Pirovano 2012). The completeness of each assembly was assessed using the BENCHMARKING UNIVERSAL SINGLE-COPY ORTHOLOGS (BUSCO) 4.0.5 tool against the Fungi dataset (Seppey et al. 2019).

*Taxon sampling and phylogenomic analyses.*—

To improve our understanding on the phylogenetic placement of the putative new species originating from *Termitomyces* combs, we performed phylogenomic analyses using both supermatrix and supertree approaches on protein sequence data. Along with the two newly generated genome sequences, we included genome data for 32 species, representing 10 currently recognized genera in the Ophiostomatales and four outgroup taxa. All additional genomes utilized in this study were downloaded from the JGI fungal genome portal MycoCosm (http://jgi.doe.gov/fungi) and NCBI GenBank (https://www.ncbi.nlm.nih.gov/genbank/) (TABLE 2).

All 34 genomes were assessed using BUSCO 4.0.5 tool against the Sordariomycota dataset (Seppey et al. 2019). Common single-copy BUSCO genes shared across all 34 genomes were identified and their amino acid sequences were extracted from the BUSCO run results. Individual gene datasets were compiled for each of the BUSCO genes and aligned with MAFFT 7.407 using the --auto option (Katoh & Standley 2013). After alignment, resulting datasets were trimmed using TRIMAL 1.4 using the -automated1 option (Capella-Gutiérrez et al. 2009). Datasets shorter than 100 amino acids after trimming were excluded from further analysis. Permutation Tail Probability (PTP) tests were conducted to identify datasets with no

phylogenetic signal and those that resulted in a P-value > 0.01 were excluded from further analyses.

*Supermatrix analyses.*

Datasets retained after filtering were concatenated into a single supermatrix using FASCONCAT 1.04 (Kück & Meusemann 2010). PARTITIONFINDER 2.1.1 was used to identify best partition scheme for the concatenated dataset (Lanfear et al. 2017). Maximum likelihood (ML) analysis was performed on the supermatrix using RAXML with 20 random ML searches followed by 100 rapid bootstrap replications under the PROTGAMMAJTT model and the partition scheme was specified according to the PARTITIONFINDER results (Stamatakis & Alachiotis 2010).

*Supertree analyses.*

Since phylogenetic reconstruction using the concatenation approach can introduce bias due to genes with strong phylogenetic signal (Shen et al. 2017), two supermatrix approaches, namely ASTRAL (Mirarab et al. 2014) and STAG (Emms et al. 2018), were also used in the phylogenomic analyses. ASTRAL identifies quartet topologies from input gene trees and searches for the consensus tree that has the maximum number of quartet topologies (Mirarab et al. 2014). STAG uses a standard "greedy" consensus method to construct a concensus tree, using distance-based trees that were derived from the input gene trees (Emms et al. 2018). Individual gene trees were generated for all BUSCO datasets using IQ-TREE 2 (Minh et al. 2020) with 1000 ultrafast bootstraps and an optimal amino acid substitution model that was automatically determined (Hoang et al. 2018). The trees obtained from IQ-TREE were used directly as input trees for STAG analysis. For ASTRAL analysis, branches in gene trees with less than 30 % bootstrap support were collapsed before they were used for species tree construction. To compare the different phylogenomic trees obtained using the three approaches, tree certainty values were calculated with RAXML using the individual ML trees

as input trees (Salichos & Rokas 2013). To estimate support for nodes in the species trees obtained using the three approaches, gene and site concordance factors were calculated in IQ-TREE 2 using the gene trees and the supermatrix respectively.

*Species descriptions.*—

*Morphology:* Ascomata were removed from sections of *Termitomyces* combs by soaking the material in 10 % KOH solution. The recovered ascomata were mounted on glass slides in 80 % lactic acid. To observe asexual structures for the various isolates, cultures were grown directly on the microscope slide using blocks of MEA. Cultures were maintained for up to 3 days at ambient room temperature before the agar blocks were removed, 80 % lactic acid was added to the structures left on the slide and then covered with a cover slip. Morphological observations were made using a Zeiss AxioScop2 microscope with a Zeiss Axiocam ICc5 camera attached (Carl Zeiss, Oberkochen, Germany). Measurements were taken for ascospores, conidia, conidiophores, conidiogenous cells, the ascomatal neck width (base and tip) and length, as well as some additional characteristics when present. Values were determined from measurements of 50 or more structures.

*Growth study:* A growth study was conducted to determine optimal growth conditions for the different lineages. Two isolates from each lineage were selected for the experiment. Agar plugs of 5 mm in diameter were excised from the actively growing edge of a 10 d old culture and placed mycelium side down onto the centre of a 90 mm MEA plate. Plates were incubated in the dark at a temperature range from 5–35 C at 5 C intervals. Colony diameter was measured daily for 10 d or until the mycelium reached the edge of the plates. Five replications were prepared for each of the isolates at each temperature treatment.

*Growth on* Termitomyces *associated media.*—

Selected isolates (TABLE 1) representing all taxa isolated from *Termitomyces* combs were grown on different media derived from the *Termitomyces* combs to determine whether compounds present in the material enhances their growth and/or sporulation.

*Fungus comb enriched medium (FCE)*: Dried *Termitomyces* comb was ground to a fine powder using a mortar and pestle. Ten grams (g) of the ground powder was suspended in 250 mL autoclaved distilled water. The bottle was placed on a rotary shaker for 6 h before the liquid was collected in 50 mL falcon tubes and centrifuged for 10 min at 8500 rpm. The supernatant was collected and sterilized using a 0.2 µm syringe filter. The filtration step was repeated once to ensure that the filtrate was free from microbial contaminants. A total of 150 mL of the filter-sterilized extract was added to 850 mL autoclaved MEA kept at 50 C to make up 1 L medium and immediately poured into Petri plates.

Termitomyces *extract medium (TE)*: *Termitomyces sp.* (LSU Accession: MT835246; ITS Accession: MT845206) cultures were grown in McCartney bottles containing 10 mL MY broth. Cultures were incubated for 2–3 wk after which the culture broth was collected by centrifugation at 8500 rpm for 10 min and sterilized using a 0.2 µm syringe filter. The filtration step was repeated once to ensure that the filtrate was free from microbial contaminants. A total of 150 mL of the broth was added to 850 mL autoclaved MEA kept at 50 C to make up 1 L medium and immediately poured into Petri dishes.

Termitomyces *mycelium medium (TM)*: The *Termitomyces* mycelium collected from the previous step was freeze-dried. A total of 10 g of freeze-dried mycelium was collected and added to 1 L MEA and macerated into the molten medium using a kitchen stick blender. After maceration, the mixture was autoclaved for 20 min at 121 C to sterilize before dispensing into Petri dishes.

Two isolates of each of the three putative new species identified in the phylogenetic analyses (TABLE 1) were selected to be grown on the various media mentioned above, as well as

MEA as a control. Agar plugs (5 mm diameter) were excised from the edges of actively growing cultures and transferred to the centres of 60 mm Petri dishes containing the different media. Three replicates plates were prepared for each isolate on each of the four media. The plates were incubated at 25 C and colony measurements were taken every day for 10 d or until isolates covered the entire plate surface. Incubation was continued for an extended period (up to two months) to observe cultures for the formation of sexual structures or changes in growth characteristics.

*Statistical analyses.*—

To determine if the different media had a significant effect on the growth of the isolates, statistical analyses were performed on the colony growth measurements taken on day eight of the growth trial using R (R Core Team, 2017; https://www.R-project.org/). Initial analyses consisted of Shapiro-Wilk and Levene tests to determine normal distribution and homogeneity of variance of the collected data. As the data were not normally distributed or homogeneous, an attempt was made to adjust the data using various methods including square root, cube root, log and Tukey's ladder of power transformations and the removal of outliers. Despite these attempts, the data could not be transformed and therefore the Kruskal-Wallis rank sum test (Kruskal & Wallis 1952) and *ad-hoc* Dunn multiple comparisons test (Dunn 1964) were conducted because they do not require normal distribution or homogeneity of the data.

**RESULTS**

*Fungal isolation and preliminary identification.*—

Isolations from ascomata on the *Termitomyces* combs yielded 49 isolates (TABLE 1). The LSU, ITS and *β-tubulin* regions were sequenced, and representatives were selected for inclusion in preliminary phylogenetic analyses. Single locus analysis of the LSU dataset (SUPPLEMENTARY FIG. 1) separated the isolates obtained from the *Termitomyces* combs

in two distinct clades (lineage A and B), separate from other species in the Ophiostomataceae. A representative isolate from each of these clades was selected for whole genome sequencing and inclusion in phylogenomic analyses.

*Genome sequencing.—*

Illumina sequencing of two isolates, one from lineage A (CMW 47058 – SAMN18275857) and one from lineage B2 (CMW 47056 – SAMN18275856), yielded 20 906 584 and 13 902 124 paired-end reads respectively. Genome assembly using the Illumina data of isolate CMW 47056 (B) yielded an assembly of 874 scaffolds (≥500 bp in size), an N50 of 55.22 Kb and a genome size of approximately 26.3 Mb, which is within the size range known for other species of Ophiostomataceae (19.5 Mb *Ceratocystiopsis brevicormi* (Vanderpool et al. 2018) – 43.8 Mb *Hawksworthiomyces lignivorus* (Wingfield et al. 2017)). Genome assembly using the Illumina data of isolate CMW 47058 (A) yielded an assembly of 398 scaffolds (≥500 bp in size), an N50 of 139.18 Kb and a genome size of approximately 16 Mb, which is the smallest genome sequenced thus far for any species in the Ophiostomataceae. BUSCO assessment using the fungi dataset showed the genome assemblies to be mostly complete, with the assembly of isolate CMW 47056 (B) being 98.4 % and the assembly of isolate CMW 47058 (A) being 90.1 % complete.

*Phylogenomic analyses.—*

To clarify the placement of lineages A and B within the Ophiostomataceae, phylogenomic analyses were performed using whole genome sequence data from 34 species, 30 of which were species in the Ophiostomatales and four outgroup taxa. A total of 1879 shared single copy BUSCO genes were identified in the genomes of all 34 investigated taxa. Ten of these were found to be shorter than 100 amino acids after aligning and trimming and thus were removed from further analyses. The Permutation Tail Probability (PTP) test then identified four additional alignments that had no phylogenetic signal with a P-value > 0.01, and these

were also removed from further analyses. Phylogenies obtained from supermatrix (RAXML) and supertree (ASTRAL and STAG) approaches differed in the placement of isolates CMW47056 (B) and CMW 47058 (A) representing two of the lineages identified from termite fungus combs within the larger Ophiostomataceae (FIG. 1). Based on maximum likelihood scores, the phylogeny obtained from RAXML analysis scored as the best of the phylogenies obtained, whereas tree certainty measures indicated that the phylogeny obtained from STAG analysis had the highest level of certainty. The RAXML phylogeny grouped isolates CMW47056 (B) and CMW 47058 (A) as sister taxa and both formed a sister clade to *Ophiostoma*. The STAG phylogeny had a similar grouping of isolates CMW47056 (B) and CMW 47058 (A), but together they formed a sister clade to both *Ophiostoma* and *Sporothrix*. The ASTRAL phylogeny grouped CMW47056 (B) as a sister taxon to *Ophiostoma* and CMW 47058 (A) as sister taxon to both *Ophiostoma* and *Sporothrix*. Other than the conflicting placement of isolates CMW47056 (B) and CMW 47058 (A) and that of *Fragosphaeria purpurea* and *Graphilbum fragrans*, the placement of the remaining investigated species and genera in the Ophiostomataceae was consistent in all phylogenomic trees.

*Phylogenetic analyses.*—

Single locus phylogenetic analyses the of ITS and *β-tubulin* regions were used to determine species-level taxonomic assignment of isolates. Isolates of lineage A formed a single, well-supported clade in both the LSU and ITS analyses (FIG. 2A; SUPPLEMENTARY FIG. 1). Despite numerous attempts using different temperatures and primer pairs, we were unable to amplify the *β-tubulin* region for isolates in lineage A. Isolates of lineage B formed a single clade in the LSU analyses (SUPPLEMENTARY FIG. 1) but formed two well supported sub-clades (lineage B1 and lineage B2) in both the ITS and *β-tubulin* analyses (FIG. 2 A, B). Using the *β-tubulin* gene map compiled by Yin et al. (2015) we determined that lineage B1 has an intron arrangement of 2/-/-/5 and lineage B2 an arrangement of 2/3/-/5. The distinct

intron arrangements for lineage B1 and B2, along with morphological differences between isolates residing in the two lineages discussed in the Taxonomy section, provides support for their separation as two distinct species.

**TAXONOMY**

Based on phylogenetic and phylogenomic analyses, the isolates from *Termitomyces* combs separated into three lineages (lineages A, B1 and B2), each distinct from each other and from all other known species in the Ophiostomataceae. Based on their unique niche and phylogenetic placement within the various analyses, two new genera are introduced in the Ophiostomataceae to accommodate the three new species revealed by the different lineages.

*Lineage A.—*

***Chrysosphaeria*** W.J. Nel, Z.W. De Beer, T.A. Duong gen. nov.

MycoBank no: 837564

*Etymology:* From Latin chryso-, golden, and -sphaera, sphere or orb, referring to the light colour of the ascoma bases in the type species.

*Diagnosis:* Distinguished from all other related genera of the Ophiostomatales due the unique morphology of the ascomata. Throughout their development, these structures remain golden brown in colour and the ascomatal necks retain their flexibility (i.e. ability to bend in different directions without breaking).

*Type species:* ***Chrysosphaeria jan-nelii*** W.J. Nel, Z.W. De Beer & T.A. Duong sp. nov. FIG. 3.

MycoBank no: 837566

*Typification:* SOUTH AFRICA. LIMPOPO PROVINCE: Mookgophong, Amsterdam farm, ascomata embedded in *Termitomyces* fungal comb of *M. natalensis*, Feb 2015, *W.J. Nel* (**holotype** PREM 63088). Living ex-type culture CMW 47058 = CBS 141570. GenBank: LSU= MT637006; ITS = MT637038; *β-tubulin* = MT649128.

*Etymology:* named for the late Professor J. J. C. Nel (1933-2019), a South African entomologist who worked on termites, grandfather of the first author and from whom she drew significant inspiration.

*Description: Sexual state*. *Ascomatal bases in culture* light to golden brown, globose, (108–)129–171(–189) µm in diameter, ornamented with short hyaline to lightly pigmented hairs. *Ascomatal necks* light brown, tapering and becoming hyaline towards apex, flexible, (309–)502–771(–989) µm long, (28–)35–48(–56) µm wide at base, (11–)13–18(–22) µm wide at apex. *Ostiolar hyphae* present, slightly divergent, hyaline. *Asci* not seen. *Ascospores* produced in slimy droplet at apex of neck, hyaline, short cylindrical to bean shaped, aseptate, no sheath, (3.0–)3.5–4.5(–5.0) µm x (1.0–)1.5–2 µm. *Asexual state. Sporothrix*-like. *Conidiophores* hyaline, micronematous, (24–)38–85(–104) µm long. *Conidiogenous cells* denticulate, hyaline, (5–)11–39 µm. *Primary conidia* hyaline, aseptate, oblong, (9.0–)10.0–12.5(–14.5) µm x (3.0–)3.5–4.0(–4.5) µm. *Secondary conidia* hyaline, obovoid, aseptate. *Culture characteristics*: Colonies hyaline with white aerial mycelium on MEA, mycelium mostly superficial on agar, slow growing, growing on average 40 mm in 10 d at 25 C, grows best at 25 C, no growth at 35 C. Protoperithecia sometimes visible after 1–2 mo in culture. *Additional specimens examined:* SOUTH AFRICA. LIMPOPO PROVINCE: Mookgophong, Amsterdam farm, ascomata embedded in *Termitomyces* fungal comb of *M. natalensis*, Feb 2015, *W.J. Nel* (**paratype** PREM 63087). Living culture CMW 47057 = CBS 141566. GenBank: LSU= MT637008; ITS = MT637037. SOUTH AFRICA. LIMPOPO PROVINCE: Mookgophong, Amsterdam farm, ascomata embedded in *Termitomyces* fungal comb of *M. natalensis*, Feb 2015, *W.J. Nel* (**paratype** PREM 63089). Living culture CMW 46495 = CBS 141571. GenBank: LSU= MT637007; ITS = MT637042. SOUTH AFRICA. LIMPOPO PROVINCE: Mookgophong, Amsterdam farm, ascomata embedded in *Termitomyces* fungal

comb of *M. natalensis*, Feb 2015, *W.J. Nel*. Living culture CMW 48039. GenBank: LSU= MT637009; ITS = MT637036.

*Notes:* Multiple attempts to amplify *β-tubulin* gene region from *C jan-nelii* were unsuccessful. A *β-tubulin* gene was identified from the genome sequence using a tBLASTx against the reference *β-tubulin* sequence from *Intubia oerlemansii*. Sequence comparison revealed that the *β-tubulin* gene of this species is highly divergent from other species of Ophiostomataceae. Identification of introns based on *β-tubulin* map compiled by Yin et al. (2015) showed that *C. jan-nelii* also has an intron arrangement 2/3/-/5 similar to that in isolates of *I. oerlemansii.*

*Lineage B.—*

***Intubia*** W.J. Nel, Z.W. De Beer, T.A. Duong gen. nov.

MycoBank no: 837565

*Etymology:* From the Xhosa language, Intubi for termite, recognising the source where the fungus was found.

*Diagnosis:* Distinguished from other phylogenetically related genera in the Ophiostomatales for their unique habitat with dark coloured, ascomata embedded in the substrate of termite abandoned *Termitomyces* combs

**Lineage B1**

*Type species:* ***Intubia macrotermitinarum*** W. J. Nel, Z. W. De Beer, T. A. Duong sp. nov. FIG. 4.

Mycobank no: 837567

*Typification:* SOUTH AFRICA. GAUTENG PROVINCE: Pretoria, Rietondale, Plant protection research institute, ascomata embedded in *Termitomyces* fungal comb of *M. natalensis*, Feb 2015, *W.J. Nel* (**holotype** PREM 63090). Living ex-type culture CMW 46496 = CBS 141560. GenBank: LSU = MT636994; ITS = MT637025; BT = MT649132.

*Etymology:* named refers to the termite sub-family *Macrotermitinae* to which all species of fungus-growing termites belong.

*Description: Sexual state*. *Ascomatal bases* dark brown, globose (117–)153–250(–302) µm in diameter. *Ascomatal necks* uniformly dark, often slightly curved, tapering towards apex, (1314–)745–2723(–3689) µm long, (26–)40–62(–80) µm wide at base, (10–)15–21(–25) µm wide at apex. *Ostiolar hyphae* absent. *Asci* not seen. *Ascospores* produced in slimy droplet at apex of the neck, hyaline, cylindrical, sometimes slightly curved, aseptate, no sheath, (5–)5.5–6.5(–7.0) µm x 1.5–2.0 µm. *Asexual state*. *Hyalorhinocladiella*-like. *Conidiophores* hyaline, smooth, arising singly from hyphae, micronematous, 19–67(–143) µm long. *Conidiogenous cells* smooth, (11–)18–45(–98) µm long. *Conidia* hyaline, bacilliform tapering toward one end, (6.5–)7.0–9.5(–11.0) µm x (2.0–)2.5–3.0 µm wide at thickest part, aseptate, arising from conidiophore or directly from hyphae. Secondary conidia present.

*Culture characteristics:* Colonies hyaline to whitish on MEA, mycelium superficial on agar with little aerial mycelium, slow growing, growing on average 39 mm in 10 d at 25 C, grows best at 30 C growing on average 58.6 mm in 10 d. Ascomata not observed in culture.

*Additional specimens examined*: SOUTH AFRICA. GAUTENG PROVINCE: Pretoria, Hatfield, University of Pretoria experimental farm, ascomata embedded in *Termitomyces* fungal comb of *M. natalensis*, Feb 2015, *W.J. Nel* (**paratype** PREM 63091). Living culture CMW 46492 = CBS 141561. GenBank: ITS = MT637030; *β-tubulin* = MT649129. SOUTH AFRICA. GAUTENG PROVINCE: Limpopo, Mookgophong, Amsterdam farm, ascomata embedded in *Termitomyces* fungal comb of *M. natalensis*, Feb 2015, *W.J. Nel*. Living culture

*natalensis*, Feb 2015, *W.J. Nel.* Living culture CMW 46494. GenBank: ITS = MT637061; *β-tubulin* = MT649121.

**Lineage B2**

***Intubia oerlemansii*** W.J. Nel, Z.W. De Beer & T.A. Duong sp. nov. FIG. 5.

Mycobank no: 837568

*Typification:* SOUTH AFRICA. GAUTENG PROVINCE: Pretoria, Rietondale, Plant protection research institute, ascomata embedded in *Termitomyces* fungal comb of *M. natalensis*, Feb 2015, *W.J. Nel* (**holotype** PREM 63094). Living ex-type culture CMW 47048 = CBS 141564. GenBank: ITS = MT637024, BT = MT649147.

*Etymology:* name honours Mr. Arien Oerlemans, owner of the farm, Amsterdam, near Mookgophong, Limpopo Province, South Africa where many of the fungus combs were collected.

*Diagnosis: Intubia oerlemansii* differs from the other species in the genus in that it produces two conidial forms. There is also a difference in the intron/exon regions of the *β-tubulin* gene with *I. oerlemansii* having exon three and five present and *I. macrotermitinarum* having only exon five present.

*Description: Sexual state*. *Ascomatal bases* dark brown to black, globose, (109–)135–192(–233) µm diameter. *Ascomatal necks* dark brown, uniformly dark throughout, (1137–)1393–1900(–2198) µm long, tapering towards apex, (30–)36–49(–60) µm wide at base, (8.0–)10.0–14.5(–17.5) µm wide at apex. *Ostiolar hyphae* absent. *Asci* not seen. *Ascospores* produced in slimy droplet at apex, hyaline, cylindrical, occasionally slightly curved, aseptate, no sheath, (5.0–)5.5–6.5(–7.0) µm x 1.0–1.5(–2.0) µm. *Asexual state. Sporothrix*-like. *Conidiophores* hyaline, smooth, arising singly, micronematous, (9–)13–74(–135) µm long. *Conidiogenous cells* (8–)19–34(–45) µm long, denticulate. *Conidia* of two types. *Type 1:* formed on hyphae, hyaline, round to obovoid, aseptate, (3.5–)4.5–5.5(–6.5) µm x (2.5–)3.0–4.0(–5.0) µm. *Type*

*2:* formed on conidiophores, hyaline, bacilliform, aseptate, (5.0–)6.0–7.5(–8.5) µm x (1.5–)2.0–3.0(–3.5) µm, secondary conidia present. *Culture characteristics*: Colonies hyaline to whitish on MEA, mycelium superficial on agar, little aerial mycelium present, slow growing, growing on average 36 mm in 10 d at 25 C, grows best at 30 C growing on average 50.4 mm in 10 d. Ascomata not observed in culture.

*Additional specimens examined:* SOUTH AFRICA. GAUTENG PROVINCE: Pretoria, Rietondale, Plant Protection Research Institute, ascomata embedded in *Termitomyces* fungal comb of *M. natalensis*, Feb 2015, *W.J. Nel* (**paratype** PREM 93095). Living culture CMW 47056 = CBS 141565. GenBank: LSU = MT637001; ITS = MT637034, BT = MT708983. SOUTH AFRICA. GAUTENG PROVINCE: Pretoria, Rietondale, Plant Protection Research Institute, ascomata embedded in *Termitomyces* fungal comb of *M. natalensis*, Feb 2015, *W.J. Nel* (**paratype** PREM 63098). Living culture CMW 46498 = CBS 141563. GenBank: LSU = MT940646; ITS = MT637040, BT = MT649134. SOUTH AFRICA. GAUTENG PROVINCE: Pretoria, Rietondale, Plant Protection Research Institute, ascomata embedded in *Termitomyces* fungal comb of *M. natalensis*, Feb 2015, *W.J. Nel*. Living culture CMW 47052. GenBank: LSU = MT637002; ITS = MT637029, BT = MT649151.

*Growth on* Termitomyces *associated media.—*

*Chrysosphaeria jan-nelii*: Analyses of growth rates on various media (MEA, FCE, TE, TM) using the Kruskal-Wallis rank sum test showed a significant difference in the growth on the supplemented media compared to the MEA controls for all isolates. Isolates of *C. jan-nelii* grew most rapidly on both MEA and FCE media and isolate CMW 47058 of this species had completely covered the surface of the FCE plates after eight days and, when growth measurements were assessed (FIG. 6).

There was no significant difference (Dunn's test) in the growth rate of isolate CMW 47058 on MEA vs. FCE, but a marked increase in average growth on FCE was observed for both *C.*

*jan-nelii* isolates growing, on average, at least 10 mm more than any of the isolates investigated. Isolates of *C. jan-nelii* also produced more aerial mycelium on all supplemented media tested (SUPPLEMENTARY FIG. 2). Fully developed perithecia were observed for both isolates after 18 d incubation on the FCE media. Protoperithecia was observed on MEA plates but their formation usually took between 1–2 mo and did not progress beyond this stage.

*Intubia*: Isolates of *I. macrotermitinarum* and *I. oerlemansii* had a somewhat slower growth rates compared those of *C. jan-nelii*. A significant decrease in growth rate was noted on TM media compared to the MEA control for all four isolates tested. As was observed for the isolates of *C. jan-nelii*, an increase in aerial mycelium formation was noted in both species on FCE medium (SUPPLEMENTARY FIG. 2).

**DISCUSSION**

In this study, the taxonomic placement of 49 ophiostomatalean isolates growing on *Termitomyces* combs collected from the nests of fungus-growing *M. natalensis* termites was considered. Single locus phylogenetic analyses of sequence data generated for the rDNA 28S and ITS regions, along with that of the partial *β-tubulin* gene, grouped the isolates in three distinct lineages, which were not closely related to any other species in the Ophiostomataceae. Due to uncertainty regarding the generic placement of the two main clades in the phylogeny based on conventional gene sequencing, the genome of a single isolate residing in each of these clades was sequenced to consider their generic placement in the Family. Phylogenomic analyses including the genomes of 28 representatives of the Ophiostomatales, along with two newly sequenced isolates, confirmed their placement as two distinct lineages in the Ophiostomataceae. Consequently, the two novel genera, *Chrysosphaeria* and *Intubia,* were described to accommodate them. Three novel species,

*Chrysosphaeria jan-nelii*, *Intubia macrotermitinarum*, and *I. oerlemansii*, were described in the new genera to accommodate all 49 isolates considered in this study.

Phylogenetic analyses using DNA sequences generated for three different gene regions (LSU, ITS and *β-tubulin*) showed that the genera *Chrysosphaeria* and *Intubia* reside in the Ophiostomataceae, but their placement in the Family was not clear. Uncertainty regarding appropriate generic placement, such as that found in this study, has been observed for other Ophiostomatalean genera including *Hawksworthiomyces* (De Beer et al. 2016b) and *Aureovirgo* (Van der Linde et al. 2016). Although the LSU and ITS regions are commonly used in phylogenetic analyses due to their ease of amplification and availability of reference sequence data (Schoch et al. 2012), these gene regions can be problematic in resolving higher level taxonomic relationships (Stielow et al. 2015). The availability of whole genome sequence data for a number of Ophiostomatalean species residing in a variety of different genera allowed us to adopt a phylogenomic approach to gain insights regarding the generic placement of the new genera in the Family. The decline in genome sequencing cost and the development of less computationally demanding phylogenomic analysis approaches will, in future, improve our ability to appropriately define the limits of genera and species, as has recently been shown in *Fusarium* (Geiser et al. 2020), and in the present study.

Phylogenomic analyses using supertree and supermatrix approaches yielded conflicting results regarding the placement of *Chrysosphaeria* and *Intubia* in the larger Ophiostomataceae. Despite these incongruencies, both approaches suggested that the two genera were most closely related to, but distinct from *Ophiostoma* and *Sporothrix*. Both RAXML and STAG analyses indicated that *Chrysosphaeria* and *Intubia* are sister genera, suggesting a single origin of association with fungus-growing termites. In the RAXML phylogeny, both genera grouped as sister to *Ophiostoma*, whereas in the STAG phylogeny both genera were grouped as sister to both *Ophiostoma* and *Sporothrix*. In the ASTRAL

analysis, *Intubia oerlemansii* (CMW47056) grouped as a sister taxon to *Ophiostoma* while *Chrysosphaeria jan-nelii* (CMW47058) grouped as a sister taxon basal to *Intubia*, *Ophiostoma* and *Sporothrix*. When considering the gene and site concordance factors as statistical support, the placement of *Chrysosphaeria* and *Intubia* in the STAG analysis was better supported than those from RAXML and ASTRAL.

The uncertainty regarding the generic placement was also seen for *Fragosphaeria purpurea* and *Graphilbum fragrans* when using the different analytical approaches. This problem was also observed in the phylogenomic study considering the Ophiostomatales by Vanderpool et al. (2018). Other than the uncertain placements mentioned above, the grouping of the remaining genera was consistent using the three approaches, as was also true in the phylogeny of Vanderpool et al (2018). Although we were not able to provide absolute confidence in the taxonomic placement of *Chrysosphaeria* and *Intubia*, phylogenomic analyses provided deeper insights into their position in the Ophiostomatales. If the taxonomic placements of the two new genera had relied solely on phylogenetic analyses of the LSU and ITS gene regions, *C. jan-nelii*, *I. macrotermitinarum* and *I. oerlemansii* would have been incorrectly treated as species in *Ophiostoma s.l.*

Because none of the new species identified in this study grouped with other species in the Ophiostomatales and had originated from a unique niche, growth factors relating to their termite association were considered. The fungi were shown to grow more actively on media supplemented with material from their termite associations than on control plates. Likewise, extended incubation of these isolates on media supplemented with extracts from the fungal combs resulted in formation of mature ascomata, which did not occur on any other growth medium.

Termites are actively involved in tending their monoculture *Termitomyces* combs, maintaining them free of invasive “weedy” microbial species (Moriya et al. 2005; Otani et al.

2019). Soon after the death of a colony or artificial removal of the termites from the combs, *Xylaria* and *Pseudoxylaria* spp. rapidly overgrow the *Termitomyces* combs (Visser et al. 2009, 2011). The same phenomenon was observed with the new taxa described in this study, which only emerged once the termites were no longer present. However, the origin of the inoculum of these species remains to be discovered. They could occur in the soil before construction of the termite mound or alternatively might be acquired in the foraged material brought into the mound. It is also possible that they could be associates of other fauna such as mites, which are known to be associated with termites (Eickwort 1990; Wang et al. 2002), and have been shown to have close associations with other Ophiostomatalean fungi (Hofstetter et al. 2013; Chang et al. 2020). In this regard, the discovery of two new genera of fungi closely associated with the biology of termites exposes a fascinating new area of investigation that deserves to be pursued.

## CONCLUSIONS

Ophiostomatalean fungi were discovered for the first time on the *Termitomyces* fungus combs of fungus-growing termites. Phylogenetic and phylogenomic analyses showed that these fungi represent three species residing in two novel genera of Ophiostomataceae. The Ophiostomatalean species discovered in this study appear to have had a long and specific association with termites. This emerged from the results of the phylogenomic analyses and was also consistent with their preferential growth on media containing extracts of the termite-fungus combs. These fungi appear only after termites have abandoned their combs, which is similar to other fungi that have been discovered in this unique niche. The role of these fungi in the biology of the termites or their associates remains to be explored.

## ACKNOWLEDGEMENTS

We thank Dr. Seonju Marincowitz for assistance with microscopy. This project was funded by The National Research foundation of South Africa (NRF), The University of Pretoria, the

Tree Protection Co-operative Programme (TPCP) and DSI-NRF Centre of Excellence in Plant-Health Biotechnology (CPHB), and the DSI-NRF SARChI Chair for Fungal Genomics.

**LITERATURE CITED**

Bankevich A, Nurk S, Antipov D, Gurevich AA, Dvorkin M. 2012. SPAdes: a new genome assembly algorithm and its applications to single-cell sequencing. Journal of Computational Biology 19: 455–477.

Bateman C, Huang Y-T, Simmons DR, Kasson MT, Stanley EL, Hulcr J. 2017. Ambrosia beetle *Premnobius cavipennis* (Scolytinae: Ipini) carries highly divergent ascomycotan ambrosia fungus, *Afroraffaelea ambrosiae* gen. nov. et sp. nov. (Ophiostomatales). Fungal Ecology 25: 41–49.

Benny G, Kimbrough J. 1980. A synopsis of the orders and families of Olectomycetes with keys to genera. Mycotaxon 12: 1–91.

Blanco-Ulate B, Rolshausen PE, Cantu D. 2013. Draft genome sequence of the grapevine dieback fungus *Eutypa lata* UCR-EL1. Genome Announcements 1: e00228–00213.

Boetzer M, Henkel C, Jansen H, Butler D, Pirovano W. 2011. Scaffolding pre-assembled contigs using SSPACE. Bioinformatics 27: 578–579.

Boetzer M, Pirovano W. 2012. Toward almost closed genomes with GapFiller. Genome Biology 13: R56.

Bolger AM, Lohse M, Usadel B. 2014. Trimmomatic: a flexible trimmer for Illumina sequence data. Bioinformatics 30: 2114–2120.

Cantarel BL, Korf I, Robb SM, Parra G, Ross E, Moore B, Holt C, Alvarado AS, Yandell M. 2008. MAKER: an easy-to-use annotation pipeline designed for emerging model organism genomes. Genome Research 18: 188–196.

Capella-Gutiérrez S, Silla-Martínez JM, Gabaldón T. 2009. trimAl: a tool for automated alignment trimming in large-scale phylogenetic analyses. Bioinformatics 25: 1972–1973.

Castresana J. 2000. Selection of conserved blocks from multiple alignments for their use in phylogenetic analysis. Molecular Biology and Evolution 17: 540–552.

Chang R, Duong TA, Taerum SJ, Wingfield MJ, Zhou X, De Beer ZW. 2020. Ophiostomatoid fungi associated with mites phoretic on bark beetles in Qinghai, China. IMA Fungus 11: 15.

D'Alessandro E, Giosa D, Huang L, Zhang J, Gao W, Brankovics B, Oliveira MME, Scordino F, Passo CL, Criseo G, van Diepeningen AD, Huang H, de Hoog GS. Romeo O. 2016. Draft genome sequence of the dimorphic fungus *Sporothrix pallida*, a nonpathogenic species belonging to *Sporothrix* a genus containing agents of human and feline sporotrichosis. Genome Announcements 4: e00184–00116.

De Beer ZW, Wingfield MJ. 2013. Emerging lineages in the Ophiostomatales. In: Seifert KA, De Beer ZW, Wingfield MJ, eds. The Ophiostomatoid Fungi: Expanding Frontiers [CBS Biodiversity Series vol. 12.]. Utrecht, The Netherlands: CBS-KNAW Fungal Biodiversity Centre. p. 21–46.

De Beer ZW, Seifert KA, Wingfield MJ. 2013a. The ophiostomatoid fungi: their dual position in the Sordariomycetes. In: Seifert KA, De Beer ZW, Wingfield MJ, eds. The Ophiostomatoid Fungi: Expanding Frontiers [CBS Biodiversity Series vol. 12.]. Utrecht, The Netherlands: CBS-KNAW Fungal Biodiversity Centre. p. 1–19.

De Beer ZW, Seifert KA, Wingfield MJ. 2013b. A nomenclator for Ophiostomatoid genera and species in the Ophiostomatales and Microascales. In: Seifert KA, De Beer ZW, Wingfield MJ, eds. The Ophiostomatoid Fungi: Expanding Frontiers [CBS Biodiversity Series vol. 12.]. Utrecht, The Netherlands: CBS-KNAW Fungal Biodiversity Centre. p. 261–268.

De Beer ZW, Duong TA, Barnes I, Wingfield BD, Wingfield MJ. 2014. Redefining *Ceratocystis* and allied genera. Studies in Mycology 79: 187–219.

De Beer ZW, Duong TA, Wingfield MJ. 2016a. The divorce of *Sporothrix* and *Ophiostoma*: solution to a problematic relationship. Studies in Mycology 83: 165–191.

De Beer ZW, Marincowitz S, Duong TA, Kim JJ, Rodrigues A, Wingfield MJ. 2016b. *Hawksworthiomyces* gen. nov. (Ophiostomatales), illustrates the urgency for a decision on how to name novel taxa known only from environmental nucleic acid sequences (ENAS). Fungal Biology 120: 1323–1340.

De Lima Barros MB, de Oliveira Schubach A, do Valle ACF, Galhardo MCG, Conceição-Silva F, Schubach TMP, Reis RS, Wanke B, Marzochi KBF, Conceição MJ. 2004. Cat-transmitted sporotrichosis epidemic in Rio de Janeiro, Brazil: Description of a series of cases. Clinical Infectious Diseases 38: 529–535.

De Meyer EM, De Beer ZW, Summerbell RC, Moharram A, de Hoog GS, Vismer HF, Wingfield MJ. 2008. Taxonomy and phylogeny of new wood-and soil-inhabiting *Sporothrix* species in the *Ophiostoma stenoceras-Sporothrix schenckii* complex. Mycologia 100: 647–661.

Dean RA, Talbot NJ, Ebbole DJ, Farman ML, Mitchell TK, Orbach MJ, Thon M, Kulkarni R, Xu J-R, Pan H. 2005. The genome sequence of the rice blast fungus *Magnaporthe grisea*. Nature 434: 980.

DiGuistini S, Wang Y, Liao NY, Taylor G, Tanguay P, Feau N, Henrissat B, Chan SK, Hesse-Orce U, Massoumi Alamouti S, Tsui CKM, Docking RT, Levasseur A, Haridas S, Robertson G, Birol I, Holt RA, Marra MA, Hamelin RC, Hirst M, Jones SJM, Bohlmann J, Breuil C. 2011. Genome and transcriptome analyses of the mountain pine beetle-fungal symbiont *Grosmannia clavigera*, a lodgepole pine pathogen. Proceedings of the National Academy of Sciences 108: 2504–2509.

Dunn OJ. 1964. Multiple comparisons using rank sums. Technometrics 6: 241–252.

Duong TA, De Beer ZW, Wingfield BD, Wingfield MJ. 2012. Phylogeny and taxonomy of species in the *Grosmannia serpens* complex. Mycologia 104: 715–732.

Duong TA, De Beer ZW, Winfield BD, Wingfield MJ. 2013. Characterization of the mating-type genes in *Leptographium procerum* and *Leptographium profanum*. Fungal Biology 117: 411–421.

Edler D, Klein J, Antonelli A, Silvestro D. 2019. raxmlGUI 2.0 beta: a graphical interface and toolkit for phylogenetic analyses using RAxML. BioRxiv 800912.

Eickwort GC. 1990. Associations of mites with social insects. Annual Review of Entomology 35: 469-488.

Emms D, Kelly S. 2018. STAG: species tree inference from all genes. BioRxiv 267914.

Flutre T, Duprat E, Feuillet C, Quesneville H. 2011. Considering transposable element diversification in *de novo* annotation approaches. PLOS ONE 6: e16526.

Forgetta V, Leveque G, Dias J, Grove D, Lyons R, Genik S, Wright C, Singh S, Peterson N, Zianni M, Kieleczawa J, Steen R, Perera A, Bintzler D, Adams S, Hintz W, Jacobi V, Bernier L, Levesque R, Dewar K. 2013. Sequencing of the Dutch elm disease fungus genome using the Roche/454 GS-FLX Titanium System in a comparison of multiple genomics core facilities. Journal of Biomolecular Techniques 24: 39–49.

Galagan JE, Calvo SE, Borkovich KA, Selker EU, Read ND, Jaffe D, FitzHugh W, Ma L-J, Smirnov S, Purcell S, Rehman B, Elkins T, Engels R, Wang S, Nielsen CB, Butler J, Endrizzi M, Qui D, Ianakiev P, Bell-Pedersen D, Nelson M, Werner-Washburne M, Selitrennikoff CP, Kinsey JA, Braun EL, Zelter A, Schulte U, Kothe GO, Jedd G, Mewes W, Staben C, Marcotte E, Greenberg D, Roy A, Foley K, Naylor J, Stange-Thomann N, Barrett R, Gnerre S, Kamal M, Kamvysselis M, Mauceli E, Bielke C, Rudd S, Frishman D, Krystofova S, Rasmussen C, Metzenberg RL, Perkins DD, Kroken S, Cogoni C, Macino G, Catcheside D, Li W, Pratt RJ, Osmani SA, DeSouza CPC, Glass L, Orbach MJ, Berglund JA, Voelker R,

Yarden O, Plamann M, Seiler S, Dunlap J, Radford A, Aramayo R, Narvig DO, Alex LA, Mannhaupt G, Ebbole DJ, Freitag M, Paulsen I, Sachs MS, Lander ES, Nusbaum C, Birren B. 2003. The genome sequence of the filamentous fungus *Neurospora crassa*. Nature 422: 859–868.

Gardes M, Bruns TD. 1993. ITS primers with enhanced specificity for basidiomycetes-application to the identification of mycorrhizae and rusts. Molecular Ecology 2: 113–118.

Geiser DM, Al-Hatmi A, Aoki T, Arie T, Balmas V, Barnes I, Bergstrom GC, Bhattacharyya MKK, Blomquist CL, Bowden R, Brankovics B, Brown DW, Burgess LW, Bushley K, Busman M, Cano-Lira JF, Carrillo JD, Chang HX, Chen CY, Chen W, Chilvers MI, Chulze SN, Coleman JJ, Cuomo CA, de Beer ZW, de Hoog GS, Del Castillo-Múnera J, Del Ponte E, Diéguez-Uribeondo J, Di Pietro A, Edel-Hermann V, Elmer WH, Epstein L, Eskalen A, Esposto MC, Everts KL, Fernández-Pavía SP, da Silva GF, Foroud NA, Fourie G, Frandsen RJN, Freeman S, Freitag M, Frenkel O, Fuller KK, Gagkaeva T, Gardiner DM, Glenn AE, Gold S, Gordon T, Gregory NF, Gryzenhout M, Guarro J, Gugino B, Gutiérrez S, Hammond-Kosack K, Harris LJ, Homa M, Hong CF, Hornok L, Huang JW, Ilkit M, Jacobs A, Jacobs K, Jiang C, Jimenez-Gasco MDM, Kang S, Kasson MT, Kazan K, Kennell JC, Kim H, Kistler HC, Kuldau GA, Kulik T, Kurzai O, Laraba I, Laurence MH, Lee TY, Lee YW, Lee YH, Leslie JF, Liew ECY, Lofton LW, Logrieco A, Sánchez López-Berges M, Luque AG, Lysøe E, Ma LJ, Marra RE, Martin FN, May SR, McCormick S, McGee CT, Meis JF, Migheli Q, Mohamed Nor NMI, Monod M, Moretti A, Mostert D, Mulé G, Munaut F, Munkvold GP, Nicholson P, Nucci M, O'Donnell K, Pasquali M, Pfenning LH, Prigitano A, Proctor R, Ranque S, Rehner S, Rep M, Rodríguez-Alvarado G, Rose LJ, Roth MG, Ruiz-Roldán C, Saleh AA, Salleh B, Sang H, Scandiani M, Scauflaire J, Schmale D 3, Short DP, Šišić A, Smith J, Smyth CW, Son H, Spahr E, Stajich JE, Steenkamp E, Steinberg C, Subramaniam R, Suga H, Summerell BA, Susca A, Swett CL, Toomajian C, Torres-Cruz TJ, Tortorano AM,

Urban M, Vaillancourt LJ, Vallad GE, van der Lee T, Vanderpool D, van Diepeningen AD, Vaughan M, Venter E, Vermeulen M, Verweij PE, Viljoen A, Waalwijk C, Wallace EC, Walther G, Wang J, Ward T, Wickes B, Wiederhold NP, Wingfield MJ, Wood AKM, Xu JR, Yang XB, Yli-Matilla T, Yun SH, Zakaria L, Zhang H, Zhang N, Zhang S, Zhang X. 2020. Phylogenomic analysis of a 55.1 kb 19-gene dataset resolves a monophyletic *Fusarium* that includes the *Fusarium solani* Species Complex. Phytopathology. (10.1094/PHYTO-08-20-0330-LE).

Glass NL, Donaldson GC. 1995. Development of primer sets designed for use with the PCR to amplify conserved genes from filamentous ascomycetes. Applied and Environmental Microbiology 61: 1323–1330.

Haridas S, Wang Y, Lim L, Massoumi Alamouti S, Jackman S, Docking R, Robertson G, Birol I, Bohlmann J, Breuil C. 2013. The genome and transcriptome of the pine saprophyte *Ophiostoma piceae*, and a comparison with the bark beetle-associated pine pathogen *Grosmannia clavigera*. BMC Genomics 14: 373.

Harrington T, Aghayeva D, Fraedrich S. 2010. New combinations in *Raffaelea*, *Ambrosiella*, and *Hyalorhinocladiella*, and four new species from the redbay ambrosia beetle, *Xyleborus glabratus*. Mycotaxon 111: 337–361.

Hausner G, Reid J, Klassen G. 1993. On the phylogeny of *Ophiostoma*, *Ceratocystis* s.s., and *Microascus*, and the relationships within *Ophiostoma* based on partial ribosomal DNA sequences. Canadian Journal of Botany 71: 1249-1265.

Hawksworth D, Crous P, Redhead S, Reynolds D, Samson R, Seifert KA, Taylor J, Wingfield M, Abaci Ö, Aime C. 2011. The Amsterdam declaration on fungal nomenclature. IMA Fungus 2: 105–111.

Hoang DT, Chernomor O, von Haeseler A, Minh BQ, Vinh LS. 2017 UFBoot2: Improving the Ultrafast Bootstrap Approximation. Molecular Biology and Evolution 35: 518-522.

Hofstetter RW, Moser J, Blomquist S. 2013. Mites associated with bark beetles and their hyperphoretic Ophiostomatoid fungi. In: Seifert KA, De Beer ZW, Wingfield MJ, eds. The Ophiostomatoid Fungi: Expanding Frontiers [CBS Biodiversity Series vol. 12.]. Utrecht, The Netherlands: CBS-KNAW Fungal Biodiversity Centre. p. 165–176.

Huang L, Gao W, Giosa D, Criseo G, Zhang J, He T, Huang X, Sun J, Sun Y, Huang J, Zhang Y, Brankovics B, Scordino F, D'Alessandro E, van Diepeningen A, de Hoog S, Huang H, Romeo O. 2016. Whole-genome sequencing and *in silico* analysis of two strains of *Sporothrix globosa*. Genome Biology and Evolution 8: 3292–3296.

Jacobs K, Wingfield M, Wingfield B. 2001. Phylogenetic relationships in *Leptographium* based on morphological and molecular characters. Canadian Journal of Botany 79: 719–732.

Jeon J, Kim K-T, Song H, Lee GW, Cheong K, Kim H, Choi G, Lee YH, Stewart JE, Klopfenstein NB, Kim MS. 2017. Draft genome sequence of the fungus associated with oak wilt mortality in South Korea *Raffaelea quercus-mongolicae* KACC44405. Microbiology Resource Announcements 5: e00797–00717.

Katoh K, Standley D. 2013. MAFFT multiple sequence alignment software version 7: Improvements in performance and usability. Molecular Biology and Evolution 30: 772–780.

Khoshraftar S, Hung S, Khan S, Gong Y, Tyagi V, Parkinson J, Sain M, Moses AM, Christendat D. 2013. Sequencing and annotation of the *Ophiostoma ulmi* genome. BMC Genomics 14: 162.

Kirisits T. 2013. Dutch elm disease and other *Ophiostoma* diseases. In: Gonthier P, Nicolotti G, eds. Infectious Forest Diseases. CABI Publishing. p. 256–282.

Kruskal WH, Wallis WA. 1952. Use of ranks in one-criterion variance analysis. Journal of the American Statistical Association 47: 583–621.

Kück P, Meusemann K. 2010. FASconCAT: Conveniet handling of data matrices. Molecular Phylogenetics and Evolution 56: 1115-1118.

Lah L, Löber U, Hsiang T, Hartmann S. 2017. A genomic comparison of putative pathogenicity-related gene families in five members of the Ophiostomatales with different lifestyles. Fungal Biology 121: 234–252.

Lanfear R, Frandsen PB, Wright AM, Senfeld T, Calcott B. 2017. PartitionFinder 2: new methods for selecting partitioned models of evolution for molecular and morphological phylogenetic analyses. Molecular Biology and Evolution 34: 772–773.

Liu F, Chen S, Ferreira MA, Chang R, Sayari M, Kanzi AM, Wingfield BD, Wingfield MJ, Pizarro D, Crespo A. 2019. Draft genome sequences of five *Calonectria* species from *Eucalyptus* plantations in China, *Celoporthe dispersa*, *Sporothrix phasma* and *Alectoria sarmentosa*. IMA Fungus 10: 1–13.

Lomsadze A, Ter-Hovhannisyan V, Chernoff YO, Borodovsky M. 2005. Gene identification in novel eukaryotic genomes by self-training algorithm. Nucleic Acids Research 33: 6494–6506.

Malloch DW, Blackwell M. 1993. Dispersal biology of the Ophiostomatoid fungi. In: Wingfield MJ, Seifert KA, Webber J, eds. *Ceratocystis* and *Ophiostoma:* Taxonomy, Ecology and Pathogenicity. St. Paul, Minnesota: APS Press. p. 195–206.

Massoumi Alamouti S, Tsui CK, Breuil C. 2009. Multigene phylogeny of filamentous ambrosia fungi associated with ambrosia and bark beetles. Mycological Research 113: 822–835.

Masuya H, Manabe R-i, Ohkuma M, Endoh R. 2016. Draft genome sequence of *Raffaelea quercivora* JCM 11526, a Japanese oak wilt pathogen associated with the platypodid beetle, *Platypus quercivorus*. Microbiology Resource Announcements 4: e00755–00716.

Minh BQ, Schmidt HA, Chernomor O, Schrempf D, Woodhams MD, von Haeseler A, Lanfear R. 2020 IQ-TREE 2: New models and efficient methods for phylogenetic inference in the genomic era. Molecular Biology and Evolution 37: 1530-1534.

Mirarab S, Reaz R, Bayzid MS, Zimmermann T, Swenson MS, Warnow T. 2014. ASTRAL: genome-scale coalescent-based species tree estimation. Bioinformatics 30: i541–i548.

Morales-Cruz A, Amrine KCH, Blanco-Ulate B, Lawrence DP, Travadon R, Rolshausen PE, Baumgartner K, Cantu D. 2015. Distinctive expansion of gene families associated with plant cell wall degradation, secondary metabolism, and nutrient uptake in the genomes of grapevine trunk pathogens. BMC Genomics 16: 469.

Moriya S, Inoue T, Ohkuma M, Yaovapa T, Johjima T, Suwanarit P, Sangwanit U, Vongkaluang C, Noparatnaraporn N, Kudo T. 2005. Fungal community analysis of fungus gardens in termite nests. Microbes and Environments 20: 243–252.

O'Donnell K, Cigelnik E. 1997. Two divergent intragenomic rDNA ITS2 types within a monophyletic lineage of the fungus *Fusarium* are non-orthologous. Molecular Phylogenetics and Evolution 7: 103–116.

Otani S, Challinor VL, Kreuzenbeck NB, Kildgaard S, Christensen SK, Larsen LLM, Aanen DK, Rasmussen SA, Beemelmanns C, Poulsen M. 2019. Disease-free monoculture farming by fungus-growing termites. Scientific Reports 9: 8819.

Quesneville H, Bergman CM, Andrieu O, Autard D, Nouaud D, Ashburner M, Anxolabehere D. 2005. Combined evidence annotation of transposable elements in genome sequences. PLOS Computational Biology 1: e22.

Roets F, Wingfield BD, de Beer ZW, Wingfield MJ, Dreyer LL. 2010. Two new *Ophiostoma* species from *Protea caffra* in Zambia. Persoonia: Molecular Phylogeny and Evolution of Fungi 24: 18.

Ronquist F, Huelsenbeck JP. 2003. MRBAYES 3: Bayesian phylogenetic inference under mixed models. Bioinformatics 17: 1572–1574.

Salichos L, Rokas A. 2013. Inferring ancient divergences requires genes with strong phylogenetic signals. Nature 497: 327–331.

Schoch CL, Seifert KA, Huhndorf S, Robert V, Spouge JL, Levesque CA, Chen W & the Fungal Barcoding Consortium. 2012. Nuclear ribosomal internal transcribed spacer (ITS) region as a universal DNA barcode marker for fungi. Proceedings of the National Academy of Sciences 109: 6241-6246.

Seppey M, Manni M, Zdobnov EM. 2019. BUSCO: assessing genome assembly and annotation completeness. Gene Prediction 3: 227–245.

Shen X-X, Hittinger CT, Rokas A. 2017. Contentious relationships in phylogenomic studies can be driven by a handful of genes. Nature Ecology & Evolution 1: 0126.

Silvestro D, Michalak I. 2012. raxmlGUI: a graphical front-end for RAxML. Organism Diversity and Evolution 12: 335–337.

Six DL. 2012. Ecological and evolutionary determinants of bark beetle-fungus symbioses. Insects 3: 339–366.

Spatafora JW, Blackwell M. 1994. The polyphyletic origins of Ophiostomatoid fungi. Mycological Research 98: 1–9.

Stamatakis A. 2006. RAxML-VI-HPC: maximum likelihood-based phylogenetic analyses with thousands of taxa and mixed models. Bioinformatics 22: 2688–2690.

Stanke M, Keller O, Gunduz I, Hayes A, Waack S, Morgenstern B. 2006. AUGUSTUS: ab initio prediction of alternative transcripts. Nucleic Acids Research 34: W435–W439.

Stielow JB, Levesque CA, Seifert KA, Meyer W, Iriny L, Smits D, Renfurm R, Verkley G, Groenewald M & Chaduli D. 2015. One fungus, which genes? Development and assessment of universal primers for potential secondary fungal DNA barcodes. Persoonia: Molecular Phylogeny and Evolution of Fungi 35: 242.

Tamura K, Stecher G, Peterson D, Filipski A, Kumar S. 2013. MEGA6: Molecular Evolutionary Genetics Analysis version 6.0. Molecular Biology and Evolution 30: 2725–2729.

Teixeira MM, de Almeida LGP, Kubitschek-Barreira P, Alves FL, Kioshima ES, Abadio AKR, Fernandes L, Derengowski LS, Souza RC, Ruiz JC, de Andrade NC, Paes HC, Nicola AM, Albuquerque P, Gerber AL, Martins VP, Peconick LDF, Viggiano Neto A, Chaucanez CB, Silva PA, Cunha OL, de Oliveira FFM, dos Santos TC, Barros ALN, Soares MA, de Oliveira LM, Marini MM, Villalobos-Duno H, Cunha MML, de Hoos S, da Silveira JF, Henrissat B, Nino-Vega GA, Cisalpino PS, Mora-Montes HM, Almeida SR, Stajich JE, Lopes-Bezerra LM, Vasconcelos ATR, Felipe MSS. 2014. Comparative genomics of the major fungal agents of human and animal Sporotrichosis: *Sporothrix schenckii* and *Sporothrix brasiliensis*. BMC Genomics 15: 943.

Ter-Hovhannisyan V, Lomsadze A, Chernoff YO, Borodovsky M. 2008. Gene prediction in novel fungal genomes using an ab initio algorithm with unsupervised training. Genome Research 18: 1979–1990.

Van der Linde JA, Six DL, De Beer WZ, Wingfield MJ, Roux J. 2016. Novel ophiostomatalean fungi from galleries of *Cyrtogenius africus* (Scolytinae) infesting dying *Euphorbia ingens*. Antonie van Leeuwenhoek 109: 589–601.

van der Nest MA, Bihon W, De Vos L, Naidoo K, Roodt D, Rubagotti E, Slippers B, Steenkamp ET, Wilken PM, Wilson A. 2014. Draft genome sequences of D*iplodia sapinea, Ceratocystis manginecans*, and *Ceratocystis moniliformis*. IMA Fungus 5: 135–140.

Vanderpool D, Bracewell RR, McCutcheon JP. 2018. Know your farmer: Ancient origins and multiple independent domestications of ambrosia beetle fungal cultivars. Molecular Ecology 27: 2077–2094.

Vilgalys R, Hester M. 1990. Rapid genetic identification and mapping of enzymatically amplified ribosomal DNA from several *Cryptococcus* species. Journal of Bacteriology 172: 4238–4246.

Visser AA, Kooij PW, Debets AJ, Kuyper TW, Aanen DK. 2011. *Pseudoxylaria* as stowaway of the fungus-growing termite nest: Interaction asymmetry between *Pseudoxylaria*, *Termitomyces* and free-living relatives. Fungal Ecology 4: 322–332.

Visser A, Ros V, De Beer Z, Debets A, Hartog E, Kuyper T, Laessøe T, Slippers B, Aanen D. 2009. Levels of specificity of *Xylaria* species associated with fungus- growing termites: a phylogenetic approach. Molecular Ecology 18: 553–567.

Wang C, Powell JE, O'Connor BM. 2002. Mites and nematodes associated with three subterranean termite species (Isoptera: Rhinotermitidae). Florida Entomologist 85: 499-506.

White TJ, Bruns T, Lee S, Taylor JW. 1990. Amplification and direct sequencing of fungal ribosomal RNA genes for phylogenetics. In: Innis MA, Gelfand DH, Sinsky JJ, White TJ, eds. PCR Protocols: A Guide To The Methods And Applications. New York: Academic Press. p. 315–322.

Wingfield BD, Ades PK, Al-Naemi FA, Beirn LA, Bihon W, Crouch JA, De Beer ZW, De Vos L, Duong TA, Fields CJ. 2015a. Draft genome sequences of *Chrysoporthe austroafricana, Diplodia scrobiculata, Fusarium nygamai, Leptographium lundbergii, Limonomyces culmigenus, Stagonosporopsis tanaceti,* and *Thielaviopsis punctulata*. IMA Fungus 6: 233–248.

Wingfield BD, Barnes I, de Beer ZW, De Vos L, Duong TA, Kanzi AM, Naidoo K, Nguyen HD, Santana QC, Sayari M. 2015b. Draft genome sequences of *Ceratocystis eucalypticola, Chrysoporthe cubensis, C. deuterocubensis, Davidsoniella virescens, Fusarium temperatum, Graphilbum fragrans, Penicillium nordicum,* and *Thielaviopsis musarum*. IMA Fungus 6: 493–506.

Wingfield BD, Ambler JM, Coetzee M, De Beer ZW, Duong TA, Joubert F, Hammerbacher A, McTaggart AR, Naidoo K, Nguyen HD. 2016a. Draft genome sequences of *Armillaria*

*fuscipes, Ceratocystiopsis minuta, Ceratocystis adiposa, Endoconidiophora laricicola, E. polonica* and *Penicillium freii* DAOMC 242723. IMA Fungus 7: 217–227.

Wingfield BD, Duong TA, Hammerbacher A, van der Nest MA, Wilson A, Chang R, Wilhelm de Beer Z, Steenkamp ET, Markus Wilken P, Naidoo K. 2016b. Draft genome sequences for *Ceratocystis fagacearum, C. harringtonii, Grosmannia penicillata,* and *Huntiella bhutanensis*. IMA Fungus 7: 317–323.

Wingfield BD, Berger DK, Steenkamp ET, Lim H-J, Duong TA, Bluhm BH, De Beer ZW, De Vos L, Fourie G, Naidoo K. 2017. Draft genome of *Cercospora zeina, Fusarium pininemorale, Hawksworthiomyces lignivorus, Huntiella decipiens* and *Ophiostoma ips*. IMA Fungus 8: 385–396.

Wingfield BD, Liu M, Nguyen HD, Lane FA, Morgan SW, De Vos L, Wilken PM, Duong TA, Aylward J, Coetzee MP. 2018. Nine draft genome sequences of *Claviceps purpurea* s. lat., including *C. arundinis, C. humidiphila,* and *C. cf. spartinae,* pseudomolecules for the pitch canker pathogen *Fusarium circinatum,* draft genome of *Davidsoniella eucalypti, Grosmannia galeiformis, Quambalaria eucalypti,* and *Teratosphaeria destructans*. IMA Fungus 9: 401.

Yin M, Duong TA, Wingfield MJ, Zhou X, de Beer ZW. 2015. Taxonomy and phylogeny of the *Leptographium procerum* complex, including *Leptographium sinense* sp. nov. and *Leptographium longiconidiophorum* sp. nov. Antonie van Leeuwenhoek 107: 547–563.

Zipfel RD, De Beer ZW, Jacobs K, Wingfield BD, Wingfield MJ. 2006. Multi-gene phylogenies define *Ceratocystiopsis* and *Grosmannia* distinct from *Ophiostoma*. Studies in Mycology 55: 75–97.

**Figure 1.** Phylogenomic trees obtained using A. supermatrix (RAxML) and B & C. supertree (ASTRAL and STAG) approaches. Trees were constructed from 1865 shared single copy

BUSCO genes present in all taxa investigated. Ln: maximum likelihood score. TC: tree certainty. TC-All: tree certainty including all conflicting bipartitions. Concordance factors determined using IQ-TREE 2 are presented at nodes as gene concordance factor/site concordance factor (gCF/sCF).

**Figure 2.** Bayesian inference trees derived from the analysis of A. the internal transcribed spacer and B. *β-tubulin* datasets. Bold black bands indicate posterior probabilities of 1.0, maximum likelihood (ML) and maximum parsimony (MP) bootstrap values above 75%, are indicated as ML/MP. – indicates an unsupported node in an analysis T = ex-type isolates

**Figure 3.** Morphological characteristics of the sexual and asexual structures of *Chrysosphaeria jan-nelii* sp. nov. (CMW 47058). A. Long-necked ascoma; B. Ascospores C. Hyaline apex with ostiolar hyphae; D. Ascomata on termite fungus comb with ascospores in slimy droplets; E. Mature primary conidia giving rise to secondary conidia; F. Primary conidia; G & H. Conidiogenous cell with conidia; I. pure culture on MEA. Bar: D = 200 μm; A = 100 μm; C = 20 μm; F, G, H = 10 μm; B, E = 5 μm

**Figure 4.** Morphological characteristics of sexual and asexual structures of *Intubia macrotermitinarum* sp. nov. (CMW 46496). A. Long necked ascoma; B. Ascospores; C. Apex without ostiolar hyphae; D. Ascoma on termite fungus comb with sticky drop of ascospores; E. Pure culture on MEA; F. Conidia formation on hyphae; G. Conidiophore with conidia. Bar: D = 500 μm; A = 100 μm; C = 50 μm; F, G = 10 μm; B = 5 μm

**Figure 5.** Morphological characteristics of sexual and asexual structures of *Intubia oerlemansii* sp. nov. (CMW 47056). A. Long-necked ascoma; B. Ascospores; C. Apex without osiolar hyphae; D. Ascomata on termite fungus comb with ascospores in slimy droplet; E. and G. Conidia produced on conidiophores; F. Conidia produced on hyphae; H. Pure culture on MEA. Bar: D = 500μm; A = 200 μm; C = 20 μm; E, F, G = 10 μm; B = 5 μm

**Figure 6.** Bar graphs of the average colony growth on the four different supplemented media types (MEA, FCE, TE, TM) after 8 days of incubation at 25 °C. The data is presented for this day because isolates of *Chrysosphaeria jan-nelii* had completely covered the surface of the FCE media plates and this represented the last day of measurements for the set (set refers to the entire group of five different types of media plates onto which the isolate was plated). *P*-values determined using the Kruskal-Wallis test, significances determined by the Dunn multiple comparisons test, and perithecial development observed on certain media is indicated. A. Results for isolates of *C. jan-nelii*. B. Results for isolates of *I. macrotermitinarum*. C. Results for isolates of *I. oerlemansii*.

[i] Corresponding authors: Wilma Nel: janine.nel@fabi.up.ac.za/nel.wilma2@gmail.com; Tuan Duong: tuan.duong@fabi.up.ac.za

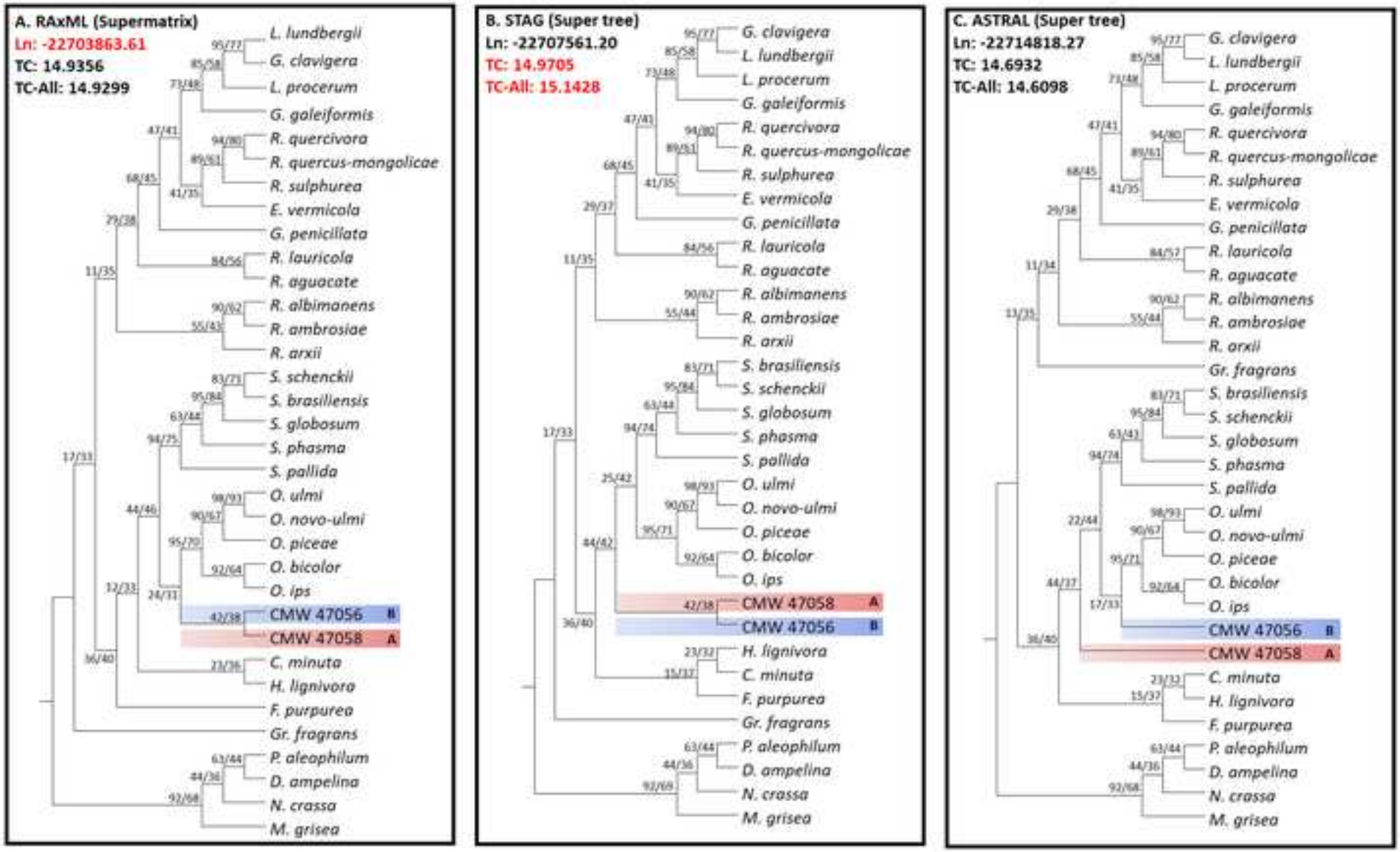

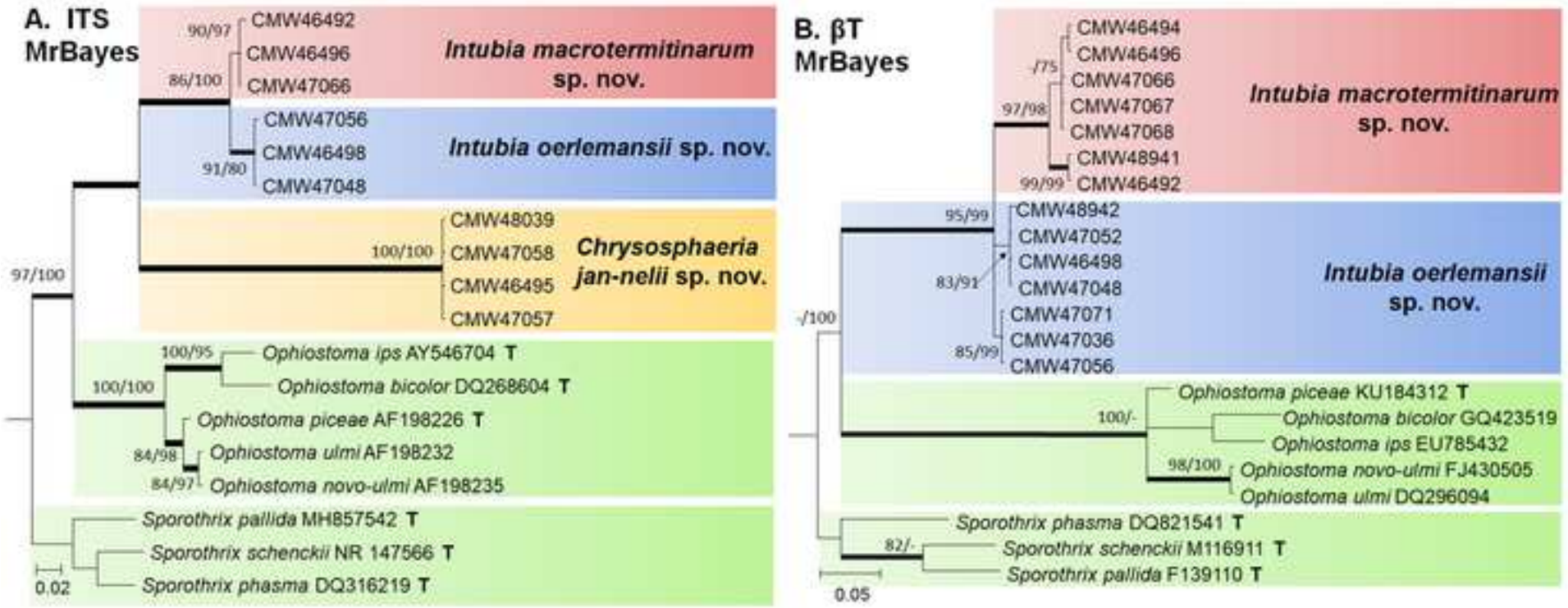

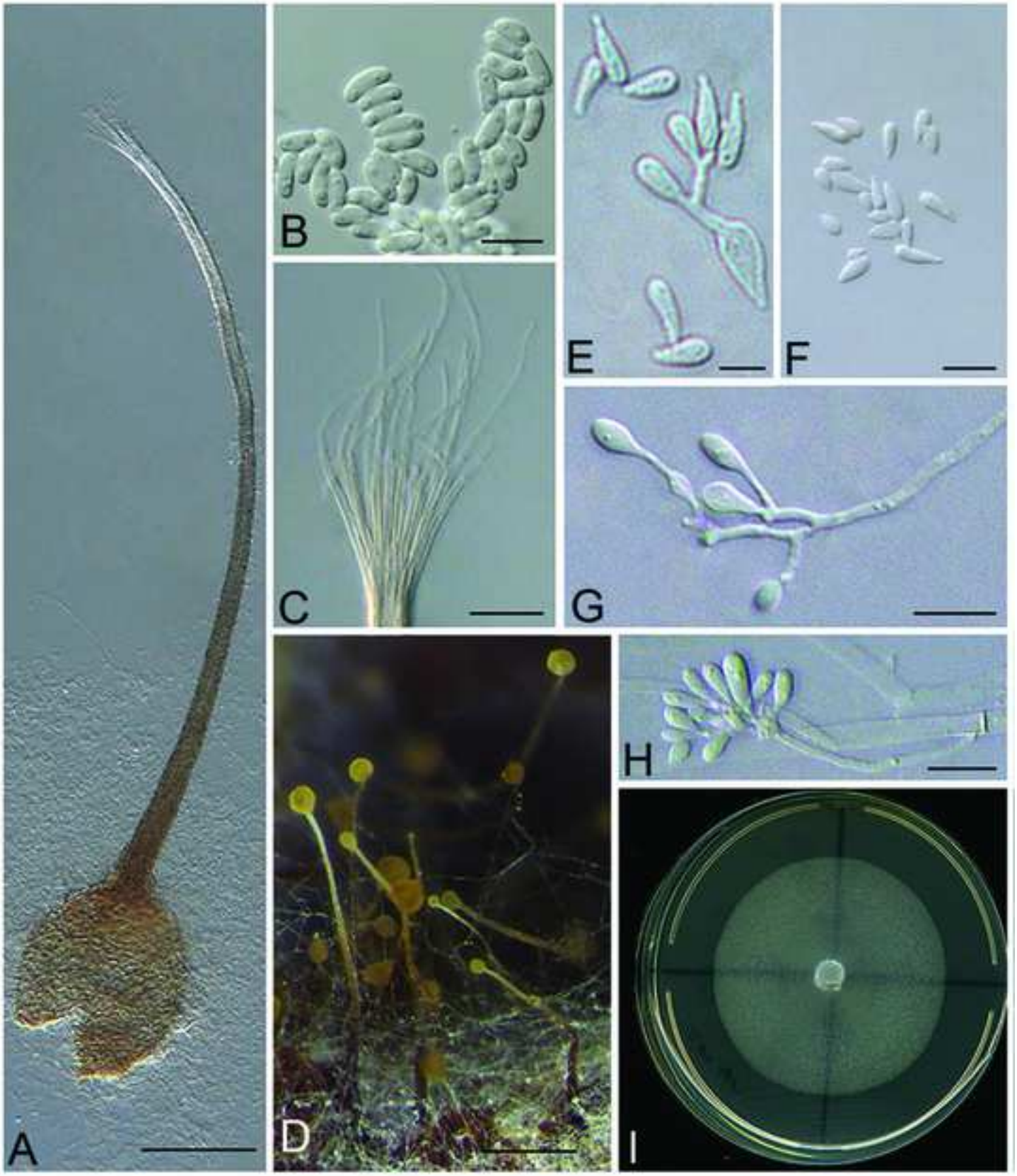

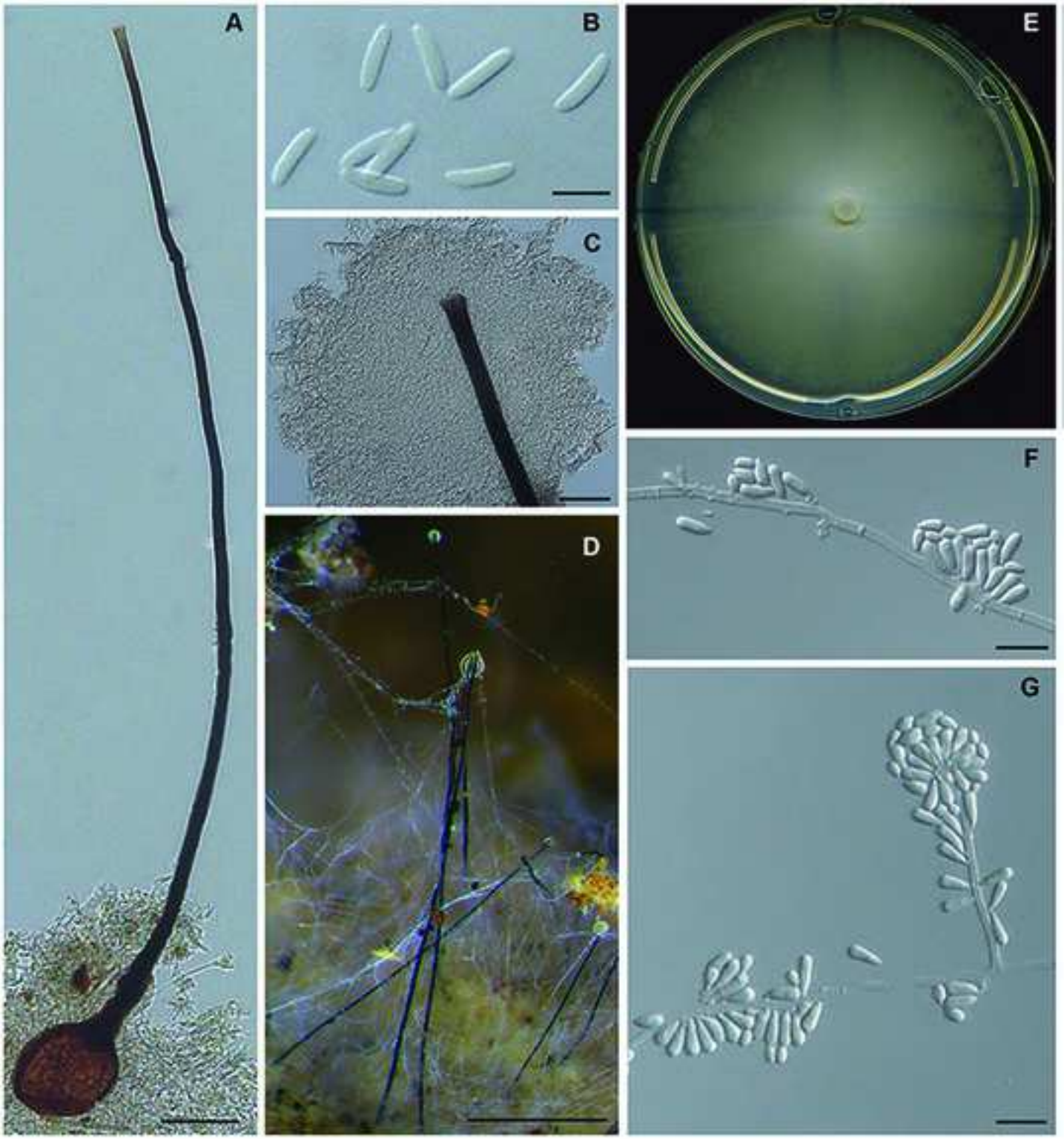

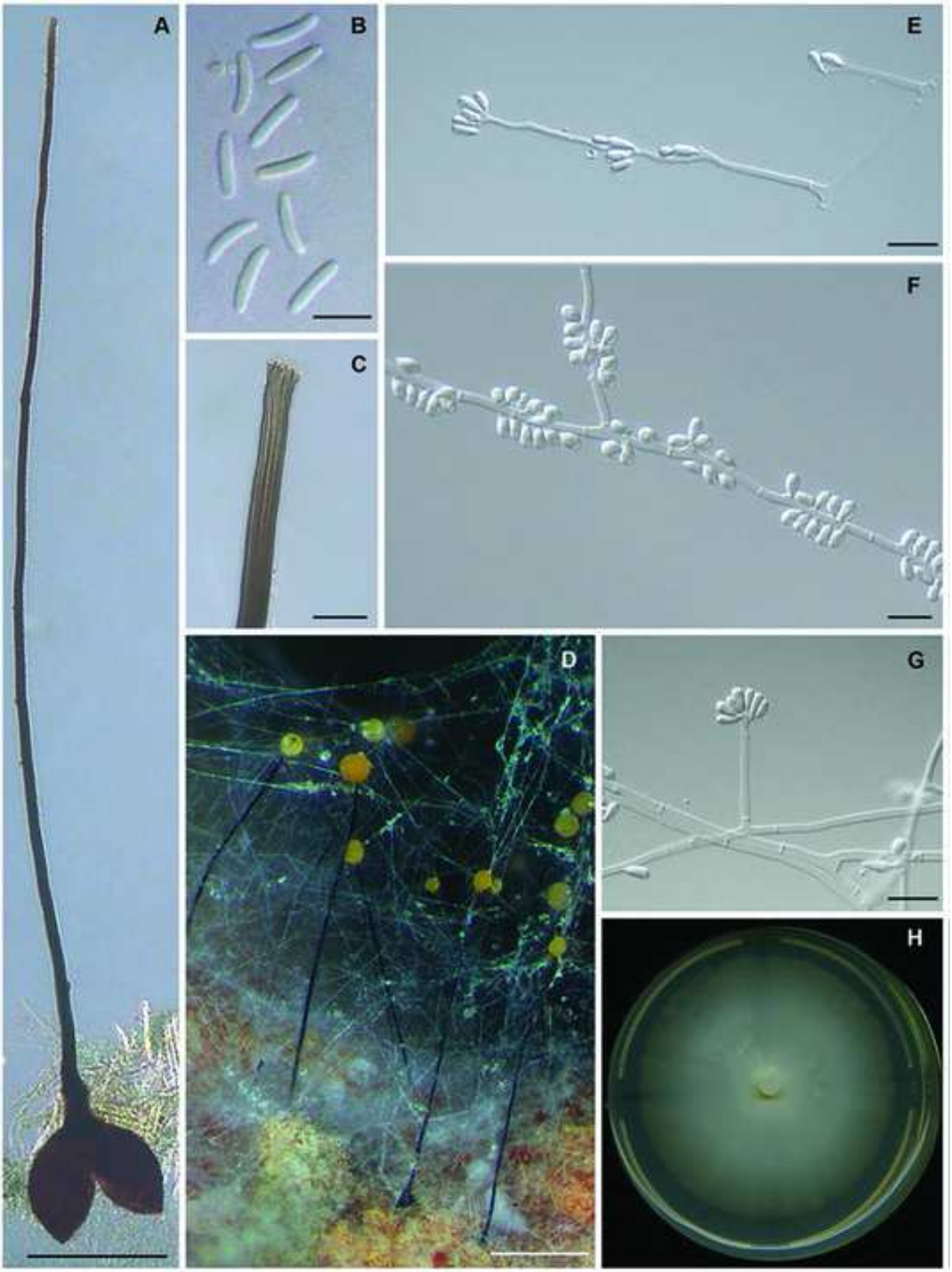

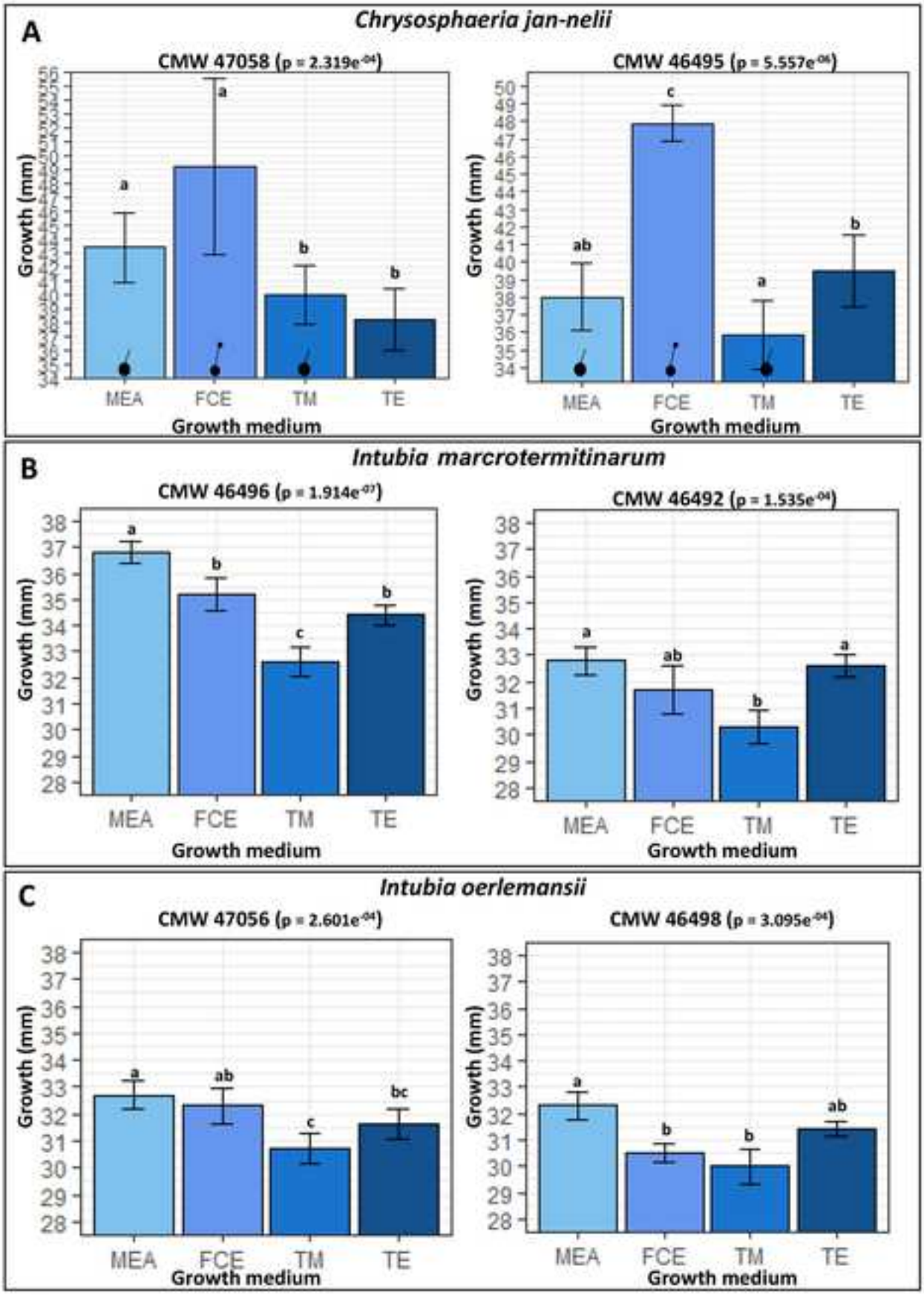

**Supplementary Figure 1.** Bayesian inference tree derived from analysis of LSU data including all major groups in the Ophiostomatales. Bold light grey bands indicate posterior probabilities above 0.95, medium grey bands indicate MP bootstrap values above 75%, and black bands indicate ML bootstrap values above 75%. Asteriks (*) indicates a node with full support from BI, ML, and MP analyses. T = ex-type isolates

**Supplementary Figure 2.** Bayesian inference tree derived from the analysis of ITS data that included species and complexes within *Ophiostoma s.l.* Bold light grey bands indicate posterior probabilities above 0.95, medium grey bands indicate MP bootstrap values above 75%, and black bands indicate ML bootstrap values above 75%. Asteriks (*) indicates a node with full support from BI, ML, and MP analyses. T = ex-type isolates

**Supplementary Figure 3.** Bayesian inference tree derived from the analysis of *β-tubulin* data that included species and complexes within *Ophiostoma s.l.* Bold light grey bands indicate posterior probabilities above 0.95, medium grey bands indicate MP bootstrap values above 75%, and black bands indicate ML bootstrap values above 75%. Asteriks (*) indicates a node with full support from BI, ML, and MP analyses. Intron/Exon composition is indicated for the various complexes and lineages on the right-hand side of the figure. T = ex-type isolates

**Supplementary Figure 4.** Representatives of the new species grown on MEA and different *Termitomyces* enriched media plates.

**Supplementary Table1.** All fungal isolates obtained and sequenced in this study.

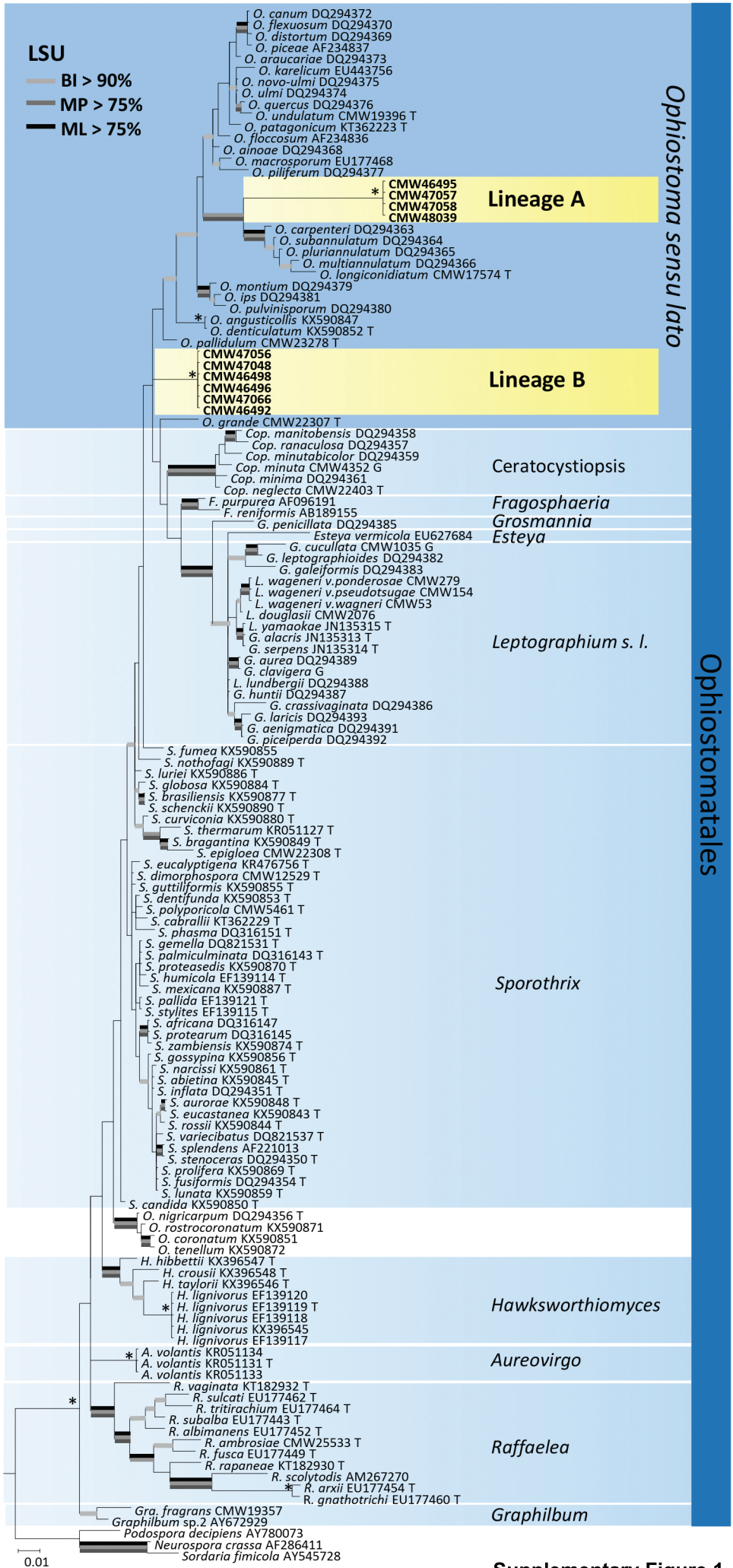


**Supplementary Figure 1**

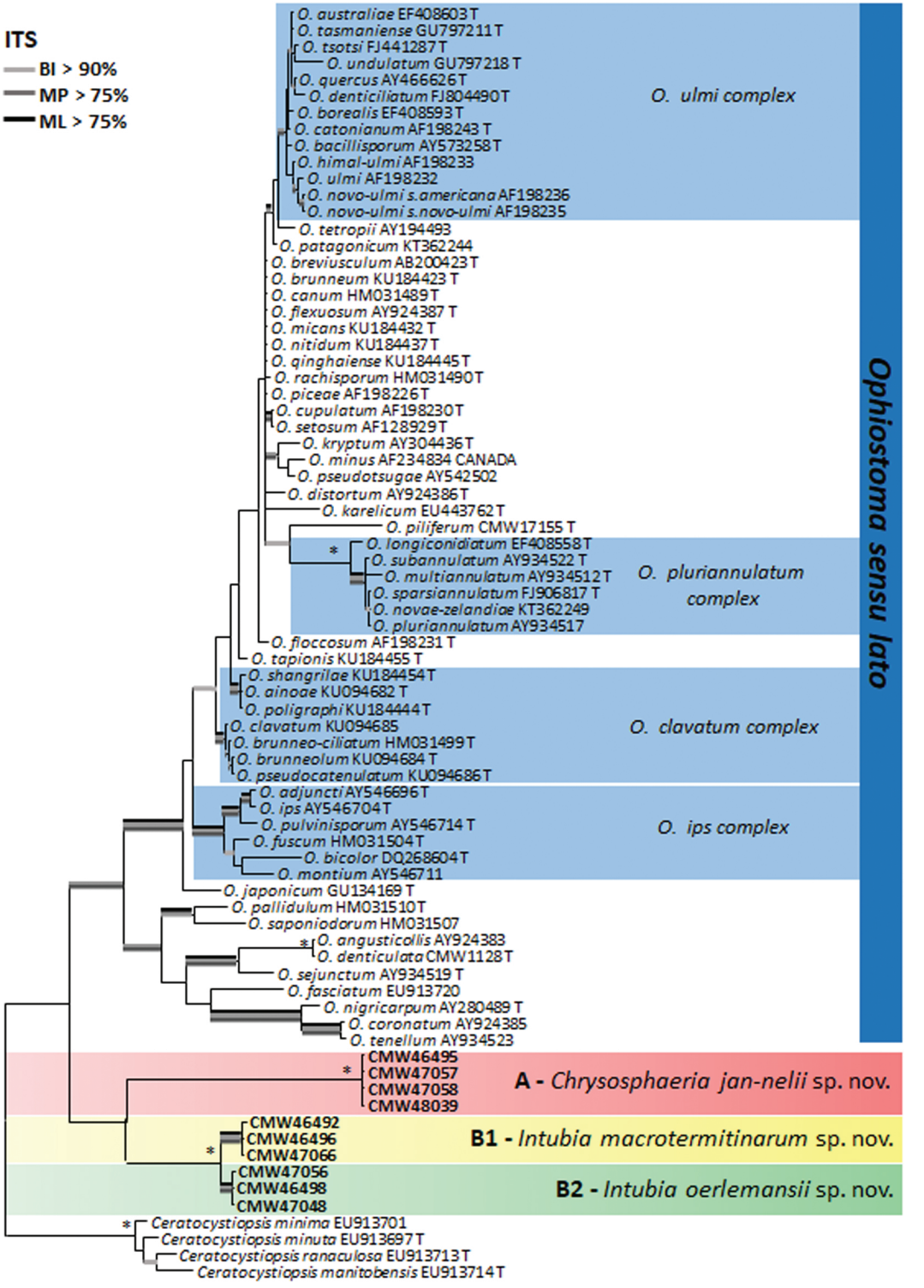
ITS
BI > 90%
MP > 75%
ML > 75%
O. australiae EF408603T
O. tasmaniense GU797211T
O. tsotsi FJ441287T
O. undulatum GU797218T
O. quercus AY466626T
O. denticiliatum FJ804490T
O. borealis EF408593T
O. catonianum AF198243T
O. bacillisporum AY573258T
O. himal-ulmi AF198233
O. ulmi AF198232
O. novo-ulmi s.americana AF198236
O. novo-ulmi s.novo-ulmi AF198235
O. ulmi complex
O. tetropii AY194493
O. patagonicum KT362244
O. breviusculum AB200423T
O. brunneum KU184423T
O. canum HM031489T
O. flexuosum AY924387T
O. micans KU184432T
O. nitidum KU184437T
O. qinghaiense KU184445T
O. rachisporum HM031490T
O. piceae AF198226T
O. cupulatum AF198230T
O. setosum AF128929T
O. kryptum AY304436T
O. minus AF234834 CANADA
O. pseudotsugae AY542502
O. distortum AY924386T
O. karelicum EU443762T
O. piliferum CMW17155T
O. longiconidiatum EF408558T
O. subannulatum AY934522T
O. multiannulatum AY934512T
O. sparsiannulatum FJ906817T
O. novae-zelandiae KT362249
O. pluriannulatum AY934517
O. pluriannulatum complex
O. floccosum AF198231T
O. tapionis KU184455T
O. shangrilae KU184454T
O. ainoae KU094682T
O. poligraphi KU184444T
O. clavatum KU094685
O. brunneo-ciliatum HM031499T
O. brunneolum KU094684T
O. pseudocatenulatum KU094686T
O. clavatum complex
O. adjuncti AY546696T
O. ips AY546704T
O. pulvinisporum AY546714T
O. fuscum HM031504T
O. bicolor DQ268604T
O. montium AY546711
O. ips complex
O. japonicum GU134169T
O. pallidulum HM031510T
O. saponiodorum HM031507
O. angusticollis AY924383
O. denticulata CMW1128T
O. sejunctum AY934519T
O. fasciatum EU913720
O. nigricarpum AY280489T
O. coronatum AY924385
O. tenellum AY934523
Ophiostoma sensu lato
CMW46495
CMW47057
CMW47058
CMW48039
A - Chrysosphaeria jan-nelii sp. nov.
CMW46492
CMW46496
CMW47066
B1 - Intubia macrotermitinarum sp. nov.
CMW47056
CMW46498
CMW47048
B2 - Intubia oerlemansii sp. nov.
Ceratocystiopsis minima EU913701
Ceratocystiopsis minuta EU913697T
Ceratocystiopsis ranaculosa EU913713T
Ceratocystiopsis manitobensis EU913714T
0.050

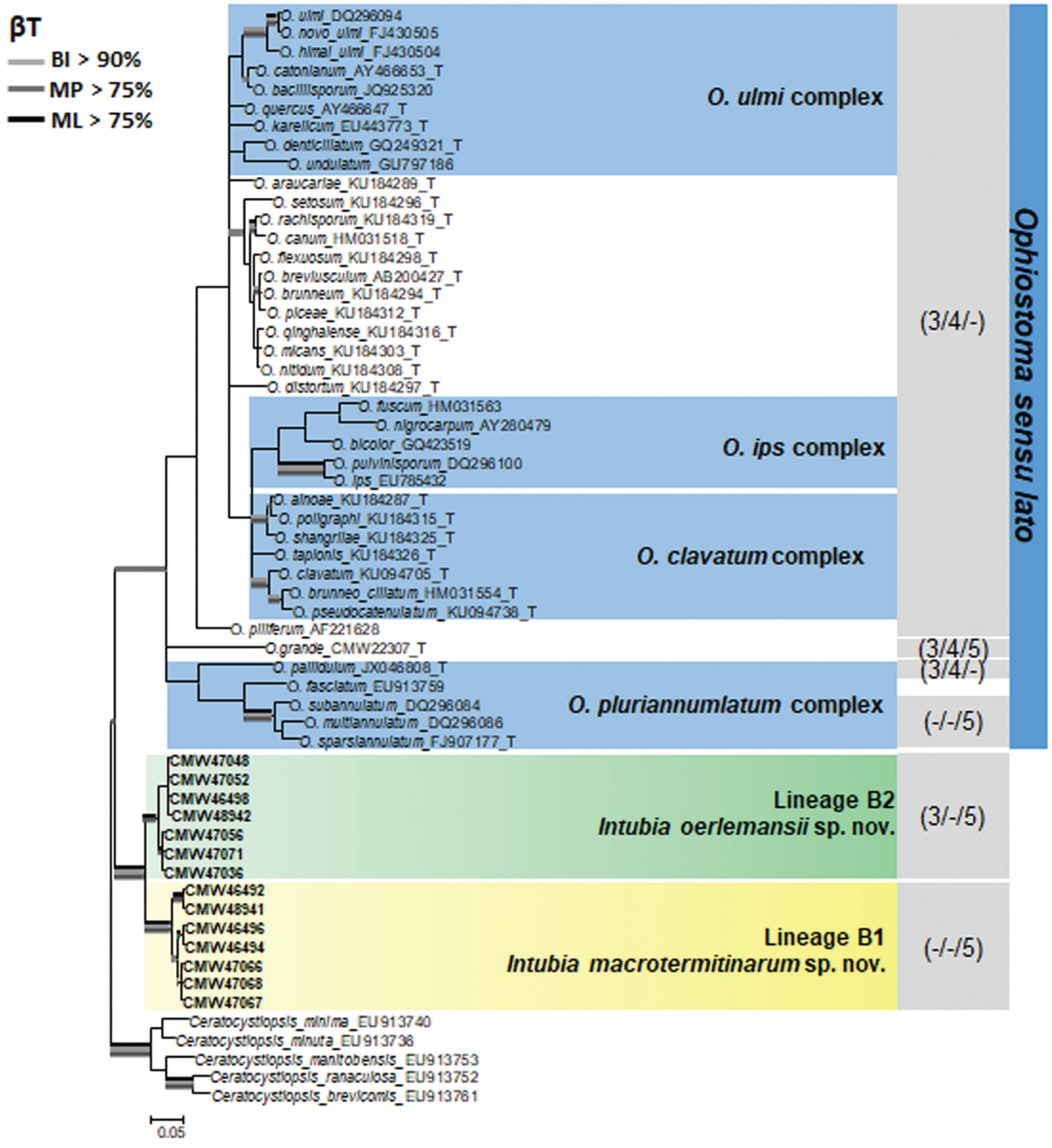
βT
BI > 90%
MP > 75%
ML > 75%
O. ulmi_DQ296094
O. novo_ulmi_FJ430505
O. himal_ulmi_FJ430504
O. catonianum_AY466653_T
O. bacillisporum_JQ925320
O. quercus_AY466647_T
O. karelicum_EU443773_T
O. denticillatum_GQ249321_T
O. undulatum_GU797186
O. ulmi complex
O. araucariae_KU184289_T
O. setosum_KU184296_T
O. rachisporum_KU184319_T
O. canum_HM031518_T
O. flexuosum_KU184298_T
O. brevisusculum_AB200427_T
O. brunneum_KU184294_T
O. piceae_KU184312_T
O. qinghaiense_KU184316_T
O. micans_KU184303_T
O. nitidum_KU184308_T
O. distortum_KU184297_T
(3/4/-)
O. fuscum_HM031563
O. nigrocarpum_AY280479
O. bicolor_GQ423519
O. pulvinisporum_DQ296100
O. ips_EU785432
O. ips complex
O. alnoae_KU184287_T
O. polligraphi_KU184315_T
O. shangrilae_KU184325_T
O. taplonis_KU184326_T
O. clavatum_KU094705_T
O. brunneo_cilliatum_HM031554_T
O. pseudocatenulatum_KU094738_T
O. clavatum complex
O. pilliferum_AF221628
O. grande_CMW22307_T
(3/4/5)
O. pallidulum_JX046808_T
(3/4/-)
O. fasciatum_EU913759
O. subannulatum_DQ296084
O. multiannulatum_DQ296086
O. sparsiannulatum_FJ907177_T
O. pluriannumlatum complex
(-/-/5)
Ophiostoma sensu lato
CMW47048
CMW47052
CMW46498
CMW48942
CMW47056
CMW47071
CMW47036
Lineage B2
Intubia oerlemansii sp. nov.
(3/-/5)
CMW46492
CMW48941
CMW46496
CMW46494
CMW47066
CMW47068
CMW47067
Lineage B1
Intubia macrotermitinarum sp. nov.
(-/-/5)
Ceratocystiopsis_minima_EU913740
Ceratocystiopsis_minuta_EU913736
Ceratocystiopsis_manitobensis_EU913753
Ceratocystiopsis_ranaculosa_EU913752
Ceratocystiopsis_brevicomis_EU913761
0.05

*Chrysosphaeria jan-nelii* (CMW 47058)

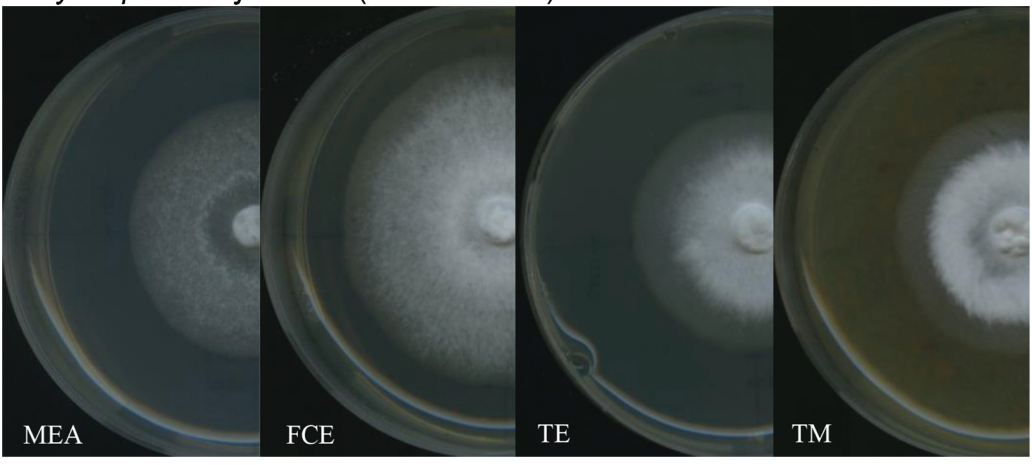


*Intubia macrotermitinarum* (CMW 46496)

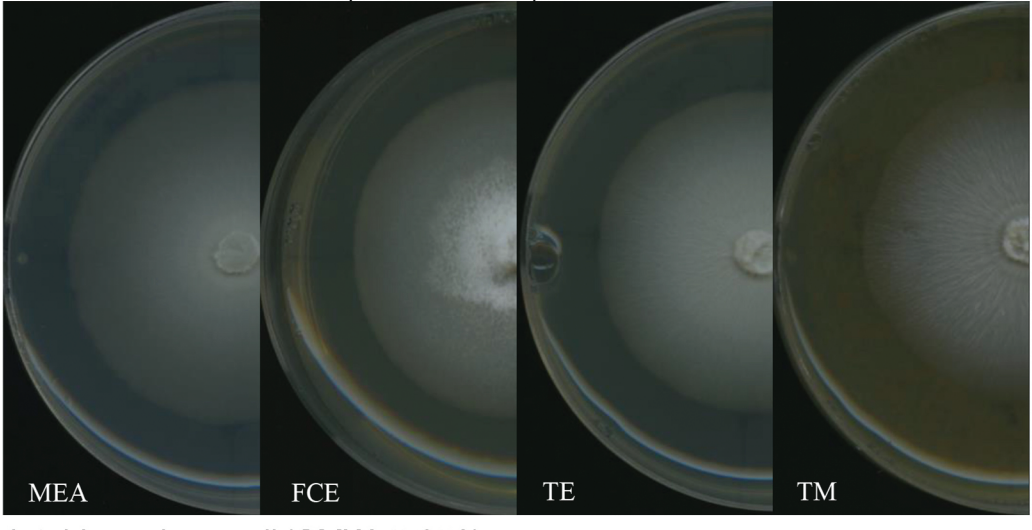


*Intubia oerlemansii* (CMW 47056)

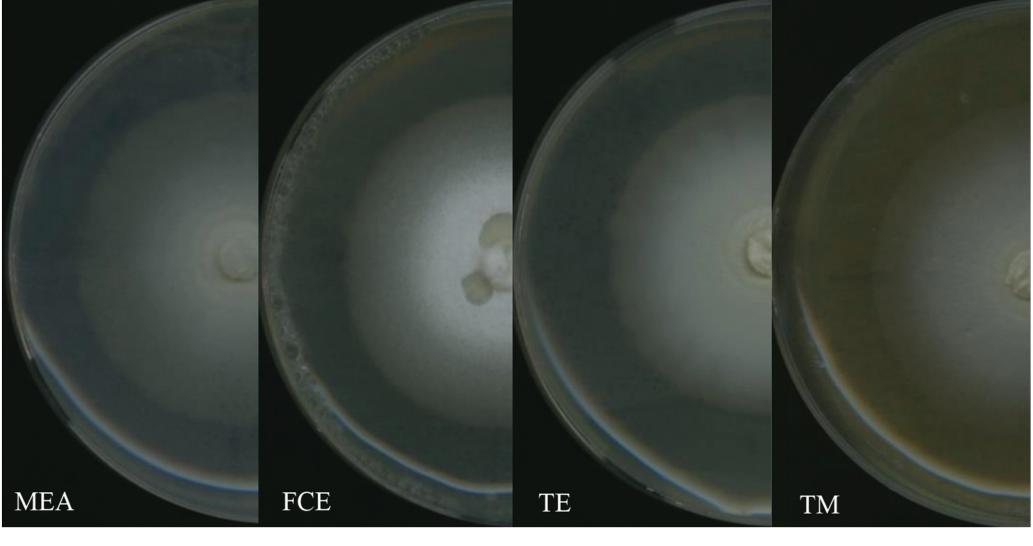

**Supplementary Table1.** All Fungal isolates obtained and sequenced in this study

| Species | Isolate number | | | Geographical Origin | Host | GenBank accession numbers | | |
|---|---|---|---|---|---|---|---|---|
| | **CMW** | **CBS** | **PREM** | | | **ITS** | **LSU** | ***βT*** |
| Lineage A: *Chrysosphaeria jan-nelii* | 48039 | | | Amsterdam farm, Mookgophong, Limpopo, SA | Fungus comb from termite mounds | MT637036 | MT637009 | |
| | 47057 | 141566 | 63087 | Amsterdam farm, Mookgophong, Limpopo, SA | Fungus comb from termite mounds | MT637037 | MT637008 | |
| | **47058[a]** | **141570** | **63088** | Amsterdam farm, Mookgophong, Limpopo, SA | Fungus comb from termite mounds | MT637038 | MT637006 | MT649128 |
| | 46495[a] | 141571 | 63089 | Amsterdam farm, Mookgophong, Limpopo, SA | Fungus comb from termite mounds | MT637042 | MT637007 | |
| Lineage B1: *Intubia macrotermitinarum* | 47040 | | | University of Pretoria, Experimental farm, Pretoria, SA | Fungus comb from termite mounds | MT637014 | | MT649139 |
| | 47041 | | | University of Pretoria, Experimental farm, Pretoria, SA | Fungus comb from termite mounds | MT637015 | | MT649140 |
| | 47042 | | 63092 | University of Pretoria, Experimental farm, Pretoria, SA | Fungus comb from termite mounds | MT637016 | | MT649141 |
| | 47043 | | | University of Pretoria, Experimental farm, Pretoria, SA | Fungus comb from termite mounds | MT637017 | | MT649142 |
| | 47044 | | | University of Pretoria, Experimental farm, Pretoria, SA | Fungus comb from termite mounds | MT637019 | MT63695 | MT649143 |
| | 47047 | | | University of Pretoria, Experimental farm, Pretoria, SA | Fungus comb from termite mounds | MT637023 | | MT649146 |
| | **46496[a]** | **141560** | **63090** | PPRI, Rietondale, Pretoria, SA | Fungus comb from termite mounds | MT637025 | MT636994 | MT649132 |
| | 47049 | | | PPRI, Rietondale, Pretoria, SA | Fungus comb from termite mounds | MT637026 | | MT649148 |
| | 47050 | | 93093 | PPRI, Rietondale, Pretoria, SA | Fungus comb from termite mounds | MT637027 | | MT649149 |
| | 47051 | | | PPRI, Rietondale, Pretoria, SA | Fungus comb from termite mounds | MT637028 | MT645590 | MT649150 |
| | 46492[a] | 141561 | 63091 | University of Pretoria, Experimental farm, Pretoria, SA | Fungus comb from termite mounds | MT637030 | | MT649129 |
| | 47053 | | | University of Pretoria, Experimental farm, Pretoria, SA | Fungus comb from termite mounds | MT637031 | MT645591 | MT649152 |
| | 47060 | | | University of Pretoria, Experimental farm, Pretoria, SA | Fungus comb from termite mounds | MT637041 | MT636992 | MT649156 |

| Species | Isolate number | | | Geographical Origin | Host | GenBank accession numbers | | |
|---|---|---|---|---|---|---|---|---|
| | **CMW** | **CBS** | **PREM** | | | **ITS** | **LSU** | ***βT*** |
| | 47063 | | | University of Pretoria, Experimental farm, Pretoria, SA | Fungus comb from termite mounds | MT637045 | | MT649159 |
| | 47064 | | | University of Pretoria, Experimental farm, Pretoria, SA | Fungus comb from termite mounds | MT637046 | | MT649160 |
| | 47065 | | | PPRI, Rietondale, Pretoria, SA | Fungus comb from termite mounds | MT637047 | MT645588 | MT649161 |
| | 47066 | | | Amsterdam farm, Mookgophong, Limpopo, SA | Fungus comb from termite mounds | MT637048 | MT636993 | MT649162 |
| | 47067 | 141562 | | Amsterdam farm, Mookgophong, Limpopo, SA | Fungus comb from termite mounds | MT637049 | MT645589 | MT649163 |
| | 47068 | | | Amsterdam farm, Mookgophong, Limpopo, SA | Fungus comb from termite mounds | MT637050 | | MT649164 |
| | 47069 | | | University of Pretoria, Experimental farm, Pretoria, SA | Fungus comb from termite mounds | MT637060 | MT636997 | MT649165 |
| | 46494 | | | PPRI, Rietondale, Pretoria, SA | Fungus comb from termite mounds | MT637061 | | MT649121 |
| | 47070 | | | PPRI, Rietondale, Pretoria, SA | Fungus comb from termite mounds | MT637062 | | MT649166 |
| | 47072 | | | University of Pretoria, Experimental farm, Pretoria, SA | Fungus comb from termite mounds | MT067064 | | MT649168 |
| | 47074 | | | PPRI, Rietondale, Pretoria, SA | Fungus comb from termite mounds | MT637066 | MT636991 | MT649170 |
| | 48941 | | | | Fungus comb from termite mounds | MT835247 | | PENDING |
| Lineage B2: | 47036 | | | PPRI, Rietondale, Pretoria, SA | Fungus comb from termite mounds | MT637010 | | MT649135 |
| *Intubia oerlemansii* | 47037 | | | PPRI, Rietondale, Pretoria, SA | Fungus comb from termite mounds | MT637011 | | MT649136 |
| | 47038 | | | PPRI, Rietondale, Pretoria, SA | Fungus comb from termite mounds | MT637012 | | MT649137 |
| | 47039 | | | PPRI, Rietondale, Pretoria, SA | Fungus comb from termite mounds | MT637013 | MT636999 | MT649138 |
| | 47045 | | | PPRI, Rietondale, Pretoria, SA | Fungus comb from termite mounds | MT637020 | MT636998 | MT649144 |
| | 46497 | | | PPRI, Rietondale, Pretoria, SA | Fungus comb from termite mounds | MT637021 | | MT649133 |
| | 47046 | | | PPRI, Rietondale, Pretoria, SA | Fungus comb from termite mounds | MT637022 | | MT649145 |

| Species | Isolate number | | | Geographical Origin | Host | GenBank accession numbers | | |
|---|---|---|---|---|---|---|---|---|
| | **CMW** | **CBS** | **PREM** | | | **ITS** | **LSU** | ***βT*** |
| | **47048** | **141564** | **63094** | PPRI, Rietondale, Pretoria, SA | Fungus comb from termite mounds | MT637024 | | MT649147 |
| | 47052 | | | PPRI, Rietondale, Pretoria, SA | Fungus comb from termite mounds | MT637029 | MT637002 | MT649151 |
| | 47054 | | | PPRI, Rietondale, Pretoria, SA | Fungus comb from termite mounds | MT637032 | | MT649153 |
| | 47055 | | 63095 | PPRI, Rietondale, Pretoria, SA | Fungus comb from termite mounds | MT637033 | MT637000 | MT649154 |
| | 47056[a] | 141565 | 63096 | PPRI, Rietondale, Pretoria, SA | Fungus comb from termite mounds | MT637034 | MT637001 | MT708983 |
| | 46493 | | 63097 | PPRI, Rietondale, Pretoria, SA | Fungus comb from termite mounds | MT637035 | | MT649130 |
| | 47059 | | | PPRI, Rietondale, Pretoria, SA | Fungus comb from termite mounds | MT637039 | | MT649155 |
| | 46498[a] | 141563 | 63098 | PPRI, Rietondale, Pretoria, SA | Fungus comb from termite mounds | MT637040 | MT940646 | MT649134 |
| | 47061 | | | PPRI, Rietondale, Pretoria, SA | Fungus comb from termite mounds | MT637043 | | MT649157 |
| | 47062 | | | PPRI, Rietondale, Pretoria, SA | Fungus comb from termite mounds | MT637044 | MT636996 | MT649158 |
| | 47071 | | | PPRI, Rietondale, Pretoria, SA | Fungus comb from termite mounds | MT637063 | | MT649167 |
| | 47073 | | | PPRI, Rietondale, Pretoria, SA | Fungus comb from termite mounds | MT637065 | | MT649169 |
| | 48942 | | | | Fungus comb from termite mounds | MT835248 | | PENDING |

[a]Isolates used in growth studies

Bold face = ex-type isolates